

Realized volatility and parametric estimation of Heston SDEs

R. Azencott ^{*} Peng Ren [†] Ilya Timofeyev [‡]

July 12, 2022

Abstract

We present a detailed analysis of the Heston model with particular emphasis on the indirect observability framework for parameter estimation in the volatility equation. Since the volatility process is not directly observable, values of parameters have to be inferred from an approximating realized volatility process. In this paper we analytically establish criteria for the optimal sub-sampling of the realized volatility process depending on the size of the averaging window. Our analytical results are supplemented by extensive numerical investigation of the Heston model. Thus, our analytical and numerical results in this paper provide practical guidelines for selecting the frequency of estimation, size of the observational samples, etc. to achieve near-optimal parameter estimation accuracy.

Keywords: Heston model, parameter estimation, indirect observability

1 Introduction

Parametric estimation of stochastic differential equations (SDEs) has been an active research area for several decades. The majority of published results focus on *Direct Observability* situations, where the observable data X_t are assumed to be generated by the SDEs themselves. But in many practical situations, the SDEs driving an *unobservable* process X_t are parametrized by a vector θ which needs to be estimated from observable data Y_t^ε which are only known to converge to X_t as $\varepsilon \rightarrow 0$. We refer to these situations as *Indirect Observability* contexts. A crucial point is then to assess estimation errors due to the use of approximate data (see, for example, [19, 28, 27, 5, 4, 12, 25]). In our papers [8, 7, 9, 11], we analyzed asymptotic consistency of parameter estimation under indirect observability in multiple contexts. In particular, in [11] we proved the asymptotic accuracy of parameter estimators based on empirical moments of indirect approximate observations, for a wide class of unobservable stationary non-Gaussian processes X_t with “fast” mixing properties. Here we extend and apply results from [11] to parameter estimation for the well known Heston SDEs [24] driving jointly the rate of returns R_t of an arbitrary asset and its squared volatility V_t . Since the volatilities V_t are not directly observable, classical observable approximations of V_t are provided by *realized volatilities* Y_t^ε computed on averaging time windows $(t - \varepsilon, t)$. Such volatility approximations have been studied for instance in [13, 16, 17, 3, 30, 6].

In this paper focused on feasible parameter estimation for the Heston volatility SDEs, we construct observable parameter estimators from the first and second order empirical moments of the realized volatility process Y_t^ε , and we analyze their L^2 -consistency as $\varepsilon \rightarrow 0$. The empirical

^{*}Department of Mathematics, University of Houston, Houston, TX 77204-3008, (razencot@math.uh.edu).

[†]Department of Mathematics, University of Houston, Houston, TX 77204-3008, (pren@math.uh.edu).

[‡]Department of Mathematics, University of Houston, Houston, TX 77204-3008, (ilya@math.uh.edu).

moments of Y_t^ε rely on explicit sub-sampling schemes which specify key computational parameters (e.g. number of points in the window $(t - \varepsilon, t)$, observational time-step, number of observations) as functions of the window size ε . Application of the general theory developed in [11] requires a substantial analytical investigation of the Heston model. We give concrete estimates for the L^q convergence speed of realized volatility Y_t^ε to true volatility V_t and we derive explicit nearly optimal sub-sampling schemes of Y_t^ε for efficient estimation of empirical moments. We compute theoretical convergence speeds for our observable estimators of the Heston SDE parameters as $\varepsilon \rightarrow 0$ and we compare them to numerically evaluated convergence speeds. To this end, we perform numerical investigation of the Heston model, through extensive simulations with $\varepsilon \rightarrow 0$. Our simulations refine and confirm our theoretical convergence rates for the realized volatilities as well as for our estimators of the Heston parameters. We thus validate asymptotically optimal ranges for the number of data points used to compute each realized volatility. Our numerical results indicate that for small but realistic values of ε , nearly optimal convergence rates of our observable parameter estimators can still be achieved with data subsampling less frequent than the theoretically prescribed rates.

The paper is organized as follows. In section 2 we discuss the return process and the realized volatility process. We introduce the Heston model in section 3. We introduce the notion of *indirect observability* in section 4, discuss analytic properties of the Heston model in sections 5, 6, and introduce moment-based parameter estimators for the volatility process in section 7. Theorem 4 in section 7 is one of our main analytical results, since it computes L^2 convergence rates for subsampled empirical moments of realized volatilities and hence yields convergence rates for our observable parameter estimators based on realized volatilities. In section 8 we discuss pragmatic discretization rates for the averaging windows $(t - \varepsilon, t)$. In sections 9 and 10 we perform an extensive numerical investigation of the Heston model, including numerical computation of the L^2 and L^4 speeds of convergence for the realized volatility process, speed of convergence of parameter estimators and empirical covariance estimators. Conclusions are presented in section 11.

2 Stochastic Volatility and SDE driven Rate of Returns

2.1 Generic stochastic volatility models

Stochastic volatility models have been applied extensively to link the continuous dynamics of an asset price A_t to its squared spot volatility $V_t > 0$, also called spot variance. As in Barndorff-Nielsen paper [13], we consider asset price processes A_t such that the *rate of return* process $dR_t = dA_t/A_t$ is driven by the SDE

$$dR_t = \mu dt + \sqrt{V_t} dZ_t, \quad (1)$$

where μ is a constant, Z_t is a standard one dimensional Brownian motion, and the squared volatility $V_t > 0$ is a square integrable continuous process. One naturally assumes that V_t is progressively measurable with respect to the increasing filtration \mathcal{F}_t , where \mathcal{F}_t is the σ -algebra of events generated by V_0 and the Z_s , $0 \leq s \leq t$. We will typically assume that $V_0 = y > 0$ is deterministic. The instantaneous *spot variance* or *squared volatility* V_t of the return rate formally verifies $V_t dt = \text{var}(dR_t)$. A classical example of this generic stochastic volatility model is provided by the well known *Heston SDEs* jointly driving R_t and V_t . Our paper will focus below on the Heston SDEs, after presenting them in section 3.

2.2 Realized Volatilities and actual volatilities

Daily or Intraday market data provide observed asset prices A_t at discretized times t , and hence discretized versions of the rate of return R_t , but the corresponding spot variances V_t cannot be directly

observed or precisely derived from market data and hence are *unobservable*. However *observable approximations* of V_t are provided by *Realized Volatilities* Y_t^ε computed from the discretized rates of returns R_s observed on the time window $(t - \varepsilon, t)$, for some small $\varepsilon > 0$.

The realized volatilities Y_t^ε are computed as follows. For each ε , partition any time window $[t - \varepsilon, t]$ into a number $J(\varepsilon)$ of equal intervals. We will *always assume* that the *partition size* $J(\varepsilon)$ verifies

$$\lim_{\varepsilon \rightarrow 0} J(\varepsilon) = +\infty.$$

The partition of $[t - \varepsilon, t]$ is defined by the $J(\varepsilon) + 1$ time-instants

$$t_k = t - \varepsilon + k\varepsilon/J(\varepsilon) \quad \text{with } k = 0, \dots, J(\varepsilon)$$

and the realized volatilities Y_t^ε are then computed by the formula

$$Y_t^\varepsilon = \frac{1}{\varepsilon} \sum_{k=1}^{J(\varepsilon)} (R_{t_k} - R_{t_{k-1}})^2. \quad (2)$$

As shown in [13], when $\varepsilon \rightarrow 0$, the realized volatilities Y_t^ε converge to V_t in L^2 . In the following theorem we extend this generic consistency result to convergence in L^q for all $q \geq 2$, with estimates of the L^q speeds of convergence. In particular, this theorem will be applied below to the Heston volatility SDE.

Theorem 1. *Consider a generic stochastic volatility model where asset prices A_t with return rate R_t and squared volatility $V_t > 0$ are linked by the SDE (1) driven by a Brownian motion Z_t . The volatilities V_t are assumed to be progressively measurable with respect to the filtration \mathcal{F}_t , where \mathcal{F}_t is generated by V_0 and the Z_s , $0 \leq s \leq t$. Fix an integer $q \geq 2$ and a time $T > 0$, and note that the following results hold for T finite as well as for $T = +\infty$. Assume that there is a constant c such that, for all $0 \leq s \leq t < T$,*

$$\|V_t\|_q \leq c \quad \text{and} \quad \|V_t - V_s\|_q \leq c(t - s)^{1/2}. \quad (3)$$

Define

$$\bar{q} = \begin{cases} q & \text{if } q \text{ is even} \\ q + 1 & \text{if } q \text{ is odd.} \end{cases}$$

Then there is a constant C such that for any partition size $J(\varepsilon)$, the realized squared volatilities Y_t^ε given by (2) verify, for all $\varepsilon > 0$

$$\|Y_t^\varepsilon - V_t\|_q \leq C \left(\frac{1}{J^{1/\bar{q}}(\varepsilon)} + \sqrt{\varepsilon} \right) \quad \text{for all } t < T. \quad (4)$$

Since $\lim_{\varepsilon \rightarrow 0} J(\varepsilon) = +\infty$, the realized volatilities Y_t^ε will hence converge in L^q to the true volatilities V_t as $\varepsilon \rightarrow 0$, at uniform speed for $t < T$. By selecting $J(\varepsilon) \equiv \varepsilon^{-\bar{q}/2}$, one can achieve an L^q -speed of convergence proportional to $\sqrt{\varepsilon}$, i.e. there is a constant $C_q = C(q, T)$ such that

$$\|Y_t^\varepsilon - V_t\|_q \leq C_q \sqrt{\varepsilon} \quad \text{for all } t < T, \quad \varepsilon > 0. \quad (5)$$

Proof. The proof is fairly technical, and hence is given in Appendix B. □

Remark: The general theorem stated above will hold when the squared volatility V_t and the rate of returns R_t are driven by classical Heston joint SDEs, because in the Heston model, V_t does indeed have Hölder continuity in L^q (namely (9)), as shown in section 3.2.

3 The Heston stochastic volatility models

3.1 The Heston joint SDEs

Heston joint SDEs [24] have been applied extensively to model the joint stochastic dynamics of asset price A_t and squared volatility V_t . The two coupled Heston SDEs driving V_t and the rate of return $dR_t = dA_t/A_t$ are of the form

$$dR_t = \mu dt + \sqrt{V_t} dZ_t, \quad (6)$$

$$dV_t = \kappa(\theta - V_t)dt + \gamma\sqrt{V_t}dB_t. \quad (7)$$

Here Z_t and B_t are standard one dimensional Brownian motions with constant instantaneous correlation $\mathbb{E}(dZ_t dB_t) = \beta dt$ where $-1 < \beta < 1$. Denote the σ -algebra generated by the Z_s , $0 \leq s \leq t$ as \mathcal{F}_t . We assume that B_t is measurable with respect to \mathcal{F}_t for all t , so that V_t will have the same property whenever $V_0 = y$ for some fixed $y > 0$. We will then sometimes use the shortcut notation

$$\mathbb{E}[U|V_0 = y] \equiv \mathbb{E}_y[U] \text{ for any random variable } U.$$

The autonomous volatility SDE (7) is parametrized by the ‘‘long run mean’’ $\theta > 0$ of V_t , by the ‘‘reversion rate’’ $\kappa > 0$, and by $\gamma > 0$ which controls the standard deviation γdt of dV_t/V_t . The parameter vector $\boldsymbol{\theta} = [\kappa, \theta, \gamma]$ must then verify the classical Feller condition [21]

$$\frac{\kappa\theta}{\gamma^2} > \frac{1}{2} \quad (8)$$

which ensures that V_t remains almost surely positive provided $V_0 > 0$. The first Heston SDE (6) is parametrized by the constant ‘‘mean return rate’’ $\mu > 0$ of the asset price, and by the correlation coefficient β .

The joint Heston processes (6), (7) are a particular case of the generic stochastic volatility models which have been used extensively to model behavior of stocks and other commodities. As discussed previously, the spot variance $\text{var}(dR_t)$ is then formally equal to $V_t dt$.

3.2 L^q -Hölder continuity for squared volatilities

To study realized volatilities for the Heston model and apply Theorem 1, we need to verify that the assumption (3) is verified for the Heston model (7). In particular, we need to show that for each $q \geq 1$ trajectories of the squared volatility process $\{V_t, t \in [0, T]\}$ generated by (7) are functions from \mathbb{R}^+ into L^q which are Hölder continuous in L^q norm with Hölder coefficient $1/2$.

Proposition 1. *Let V_t be driven by the Heston volatility SDE (7). Fix any $q \geq 1$ and assume that V_0 is deterministic, or more generally that its norm $\|V_0\|_q$ is finite. Then there is a constant C , depending only on q , $\|V_0\|_q$, and $\boldsymbol{\theta}$, such that for all $0 \leq s \leq t$, one has the uniform bounds*

$$\|V_t\|_q \leq C \quad \text{and} \quad \|V_t - V_s\|_q \leq C(t - s)^{1/2}. \quad (9)$$

Proof. The moments of V_t will be studied in details in section 6, where we prove that for each $q \geq 1$, the moments $\mathbb{E}[V_t^q]$ are finite and uniformly bounded for all $t > 0$. By construction

$$dV_t = b_t + \sigma_t dZ_t, \quad (10)$$

where the drift b_t and the squared diffusion coefficient σ_t^2 are linear functions of V_t . For each $q \geq 1$, the moments $\mathbb{E}[|b_t|^q]$ and $\mathbb{E}[|\sigma_t|^q]$ must hence remain uniformly bounded for all $t > 0$, since this is

the case for the V_t . A generic result on SDEs with coefficients bounded in L^q , such as (10), (see Proposition 3 in Appendix A) implies the existence of a constant C such that

$$\|V_t - V_s\|_q \leq C(t-s)^{1/2} \quad \text{for all } 0 \leq s \leq t,$$

which concludes the proof. \square

3.3 L^q -approximation of Heston volatilities by realized volatilities

The next result shows that for the Heston volatility SDE the realized volatilities Y_t^ε do converge to V_t in L^q as $\varepsilon \rightarrow 0$, at L^q -speed $\equiv \sqrt{\varepsilon}$, for adequately selected partition sizes $J(\varepsilon)$.

Theorem 2. *Consider the rate of returns R_t and the squared volatilities V_t driven by the joint Heston SDEs (6), (7). Realized volatilities Y_t^ε are computed from the rate of return process by formula (2), which is fully determined by the partition sizes $J(\varepsilon)$. Select and fix partition sizes $J(\varepsilon)$ such that $J(\varepsilon) \rightarrow \infty$ as $\varepsilon \rightarrow 0$. Fix any $q \geq 1$. Then, as $\varepsilon \rightarrow 0$, the process Y_t^ε converges to V_t in L^q , uniformly in $t > 0$. When $q \geq 2$ is an even integer, there is a constant c such that*

$$\|Y_t^\varepsilon - V_t\|_q \leq c \left(\frac{1}{J^{1/q}(\varepsilon)} + \varepsilon^{1/2} \right) \quad \text{for all } t > 0$$

and this L^q -speed of convergence is equivalent to $\varepsilon^{1/2}$ provided $J(\varepsilon) \sim \varepsilon^{-q/2}$.

Proof. Due to the uniform Hölder continuity in L^q of the V_t proved in Proposition 1, this is a direct corollary of Theorem 1, where the hypotheses are satisfied with $T = +\infty$. \square

4 Observable Parameters Estimators for the Heston Model

4.1 Parameter Estimation from true volatility data

To fit the Heston model to asset prices data, one needs to estimate the parameters μ, β of the SDE (6) and the parameter vector θ of the Heston volatility SDE (7). Since the volatility V_t is unobservable, the key issue in parametric estimation of the Heston model is to estimate θ (see, e.g. [10]). Consider first the ideal but unrealistic case where we are given a large finite set of N true volatilities values $\mathcal{V} = \{V_{n\Delta}\}$, sub-sampled at time intervals Δ . For processes driven by smoothly parametrized SDEs, many publications have studied parameter estimation from large data sets *actually generated* by the underlying SDEs (see for instance [1, 3, 2, 14, 20, 23, 22, 29, 26, 15], etc.). Several of these approaches rely either on Maximum Likelihood Estimators (MLEs) or on Methods of Moments.

Maximum Likelihood Estimators: For the Heston volatility SDE, the MLEs of θ have been thoroughly analyzed in [10], where they are explicitly computed from any finite set of true volatilities \mathcal{V} . Under minor parameter constraints and as $N \rightarrow \infty$, these MLEs were shown to be asymptotically consistent, and asymptotically normal when $\kappa\theta/\gamma^2 > 1$. Note that the impact of replacing the unobservable volatilities V_t by the realized volatilities Y_t^ε in the explicit MLE formulas of [10] is a quite technical task which we will complete in a future paper.

Moments based Estimators: In this paper, we will focus instead on natural *Moment Estimators* $\hat{\theta}$ of the Heston SDE parameter vector θ . Since the true squared volatilities V_t are *unobservable*, $\hat{\theta}$ is constructed as an explicit smooth function of the empirical mean and two lagged empirical covariances of the *observable* realized volatilities Y_t^ε .

4.2 Parameter estimation under indirect observability

Moments estimators approach considered in this paper falls formally within the generic *Indirect Observability* framework we introduced in [11]. In this framework, we analyze the *observable* processes Y_t^ε which, as $\varepsilon \rightarrow 0$, converge in L^4 to an *unobservable* processes X_t parametrized by a vector θ . In particular, in [11], after selecting a number of observables $N(\varepsilon)$ and a sub-sampling rate $\Delta(\varepsilon)$, the *observable estimators* $\hat{\theta}(\varepsilon)$ of θ are constructed as smooth functions of the empirical mean and a finite set of empirical lagged covariances of the observables $Y_{n\Delta(\varepsilon)}^\varepsilon, 1 \leq n \leq N(\varepsilon)$. Under a broadly applicable set of *Indirect Observability Hypotheses*, which however require X_t to be weakly stationary, we demonstrated in [11] that one can construct observable moment estimators achieving consistency as $\varepsilon \rightarrow 0$, provided $N(\varepsilon)$ and $\Delta(\varepsilon)$ are adequately selected.

Here we apply similar techniques to the following indirect observability situation - (i) the unobservable process X_t is the squared volatility process V_t , (ii) the observable Y_t^ε converging to V_t as $\varepsilon \rightarrow 0$ are the realized volatilities defined by the rate of returns process associated to V_t . Note that in the present paper the process V_t starting at a deterministic $V_0 = y > 0$ is not stationary; therefore, analytical results in the present paper require an enhancement of technical methods used previously in [11].

5 Transition Densities for squared volatilities

5.1 Explicit transition density

Consider squared volatilities V_t driven by the Heston volatility SDE (7) parametrized by θ . We will always assume that $V_0 > 0$ has finite moments of all orders, which is of course the case if V_0 is deterministic. For $T > 0$, introduce the following short-hand notations

$$\nu_T = e^{-\kappa T}, \quad r = \frac{2\kappa\theta}{\gamma^2} - 1 > 0, \quad \Lambda = \frac{2\kappa}{\gamma^2}, \quad \lambda_T = \frac{\Lambda}{1 - \nu_T}. \quad (11)$$

As shown in [18], the Markov diffusion process V_t has transition density given by

$$p(z, y) = P(V_{s+T} = z | V_s = y) = \lambda_T \left(\frac{z}{y\nu_T} \right)^{r/2} \exp(-\lambda_T(z + y\nu_T)) I_r(2\lambda_T\sqrt{zy\nu_T}), \quad (12)$$

where I_r is the modified Bessel function of the 1st kind of order r . As noted in [18], for fixed T , the linear rescaling $V_t \rightarrow 2\lambda_T V_t$ transforms the transition density $p(z, y)$ into

$$P(2\lambda_T V_T = z | 2\lambda_T V_0 = y) = p\left(\frac{z}{2\lambda_T}, \frac{y}{2\lambda_T}\right) \frac{1}{2\lambda_T} = \frac{1}{2} \left(\frac{z}{y\nu_T} \right)^{r/2} \exp(-(z + y\nu_T)/2) I_r(\sqrt{zy\nu_T}),$$

which, for each fixed y , is a *non-central χ^2 density* with non-centrality parameter $NCP(T, y) = y\nu_T$ and $DFR = 2r + 2$ degrees of freedom. Note that $DFR = 4\kappa\theta/\gamma^2 = 2\theta\Lambda$.

5.2 The stationary squared volatility process V_t

Since $\nu_T \rightarrow 0$ and $\lambda_T \rightarrow \Lambda$ as $T \rightarrow \infty$, $p(z, y)$ converges pointwise, at the speed $e^{-\kappa T}$, to the *unique stationary density* $\psi(z)$ of the autonomous Heston volatility SDE. This stationary density is given for all $z > 0$ by

$$\psi(z) = \frac{\Lambda}{\Gamma(r+1)} (\Lambda z)^r \exp(-\Lambda z). \quad (13)$$

When the initial condition V_0 is random with density ψ , all V_t have then the same density ψ , and the process V_t driven by the Heston volatility SDE becomes *strictly stationary*. Expectations with respect to this stationary diffusion will be denoted \mathbb{E}_ψ .

Note, that since $\lim_{T \rightarrow \infty} NCP(T, y) = 0$, the linear rescaling $z \rightarrow 2\Lambda z$ transforms the stationary density $\psi(z)$ into $(2\Lambda)^{-1}\psi(z/2\Lambda)$ which is a *standard* χ^2 density with $DFR = 2r + 2$ degrees of freedom.

6 Conditional Moments of squared volatilities

6.1 Moments of non-central χ^2

Let X be a random variable having a non-central χ^2 density with DFR degrees of freedom and non-centrality parameter NCP . Then, the Laplace transform $Lap(z) = \mathbb{E}(e^{zX})$ is, for $0 \leq z < 1/2$,

$$Lap(z) = (1 - 2z)^{DFR} \exp\left(NCP \frac{z}{1 - 2z}\right) = (1 - 2z)^{DFR} \sum_{n=0}^{\infty} \frac{1}{n!} (NCP)^n \left(\frac{z}{1 - 2z}\right)^n.$$

Expanding $1/(1 - 2z)^n$ as a series in z , we obtain, for a fixed DFR ,

$$Lap(z) = \sum_{q=0}^{\infty} \pi_q(NCP) \frac{z^q}{q!},$$

where the $\pi_q(NCP)$ are *polynomials* of degree q in NCP , with coefficients fully determined by DFR and q . Denote $nc\chi(q)$ and $st\chi(q)$ the respective moments of order q for the non-central χ^2 density and for the standard χ^2 density with DFR degrees of freedom. We then have the polynomial expressions

$$nc\chi(q) = \pi_q(NCP) \quad \text{and} \quad st\chi(q) = \pi_q(0). \quad (14)$$

For the first two moments of the non-central χ^2 and the standard χ^2 , one has, for instance, the following well known formulas

$$\begin{aligned} nc\chi(1) &= \pi_1(NCP) = DFR + NCP, \\ nc\chi(2) &= \pi_2(NCP) = NCP^2 + 2NCP(DFR + 2) + DFR^2 + 2DFR, \\ st\chi(1) &= DFR, \\ st\chi(2) &= DFR^2 + 2DFR. \end{aligned} \quad (15)$$

6.2 Conditional Moments of the squared volatilities

Recall that $\nu_T = e^{-\kappa T}$ and that $DFR = 2r + 2$ is determined by θ . The next proposition addresses the computation of conditional moments for V_t

$$M_q(y, T) \equiv \mathbb{E}[V_{s+T}^q \mid V_s = y] = \mathbb{E}[V_T^q \mid V_0 = y] \equiv \mathbb{E}_y[V_T^q]. \quad (16)$$

Proposition 2. *For each $q \geq 1$ and for each $y > 0$, the conditional moments $\mathbb{E}_y[V_T^q]$ remain uniformly bounded for all $T \geq 0$. There is a polynomial Q_q with coefficients depending only on q and θ , such that for all s, T and all $y > 0$,*

$$M_q(y, T) \equiv \mathbb{E}[V_{s+T}^q \mid V_s = y] = Q_q(y). \quad (17)$$

As $T \rightarrow \infty$, moments $M_q(y, T)$ converge at the exponential speed $\nu_T = e^{-\kappa T}$ to finite moments $m_q = \mathbb{E}_\psi[V_t^q]$ of the stationary diffusion V_t driven by the Heston volatility SDE.

Proof. The rescaling $V_s \rightarrow 2\lambda_T V_s$, with λ_T in (11), transforms the conditional distribution of V_{s+T} given that $V_s = y$ into a non-central χ^2 with

$$DFR = 2r + 2 = 2\theta\Lambda \quad \text{and} \quad NCP = (2\lambda_T y)\nu_T = \nu_T \frac{2\Lambda}{1 - \nu_T} y.$$

This rescaling implies, using the non-central χ^2 moments (14),

$$\begin{aligned} M_q(y, T) &= \frac{1}{(2\lambda_T)^q} \mathbb{E}[(2\lambda_T V_T)^q \mid 2\lambda_T V_0 = 2\lambda_T y] = \frac{1}{(2\lambda_T)^q} \pi_q(2\lambda_T y \nu_T) \\ &= \left[\frac{1 - \nu_T}{2\Lambda} \right]^q \pi_q \left(y \nu_T \frac{2\Lambda}{1 - \nu_T} \right). \end{aligned}$$

Define the homogeneous polynomial $H_q(a, b)$ of total degree q by

$$H_q(a, b) = a^q \pi_q(b/a), \tag{18}$$

where $\pi_q(\cdot)$ is defined by the Laplace transform introduced in section 6.1. Therefore, coefficients of H_q depend only on q and on θ . Next, we define

$$Q_q(y) = H_q \left(\frac{1 - \nu_T}{2\Lambda}, y \nu_T \right). \tag{19}$$

Since $0 \leq \nu_T \leq 1$ is a constant given by (11), the expression (19) for $Q_q(y)$ proves equation (17).

Equation (17) also implies the existence of a constant C such that

$$M_q(y, T) \leq C(1 + y)^q \quad \text{for all } T \geq 0.$$

Therefore for each $V_0 = y > 0$, moments $\mathbb{E}_y[V_T^q]$ remain bounded for all $T \geq 0$. As discussed in section 5.2, rescaling by Λ transforms the stationary density ψ into a standard χ^2 distribution, and hence stationary moments

$$m_q = \mathbb{E}_\psi[V_T^q] = \int_{y \geq 0} y^q \psi(y) dy$$

must be finite. As $T \rightarrow \infty$, both $\nu_T = e^{-\kappa T}$ and NCP tend to 0, and $\lambda_t \rightarrow \Lambda$ while DFR remains constant. Hence, due to (17), (19) the $M_q(y, T)$ converge at exponential speed ν_T to

$$m_q = \mathbb{E}_\psi[V_s^q] = H_q \left(\frac{1}{2\Lambda}, 0 \right) \equiv \pi_q(0).$$

□

6.3 Mean and Covariances of the stationary diffusion V_t

Using (15), and the appropriate rescaling of V_t by $2\lambda_T$ one easily computes the first two conditional moments of the squared volatility process starting at $y > 0$, namely

$$M_1(y, T) = \mathbb{E}_y[V_T] = (1 - \nu_T)\theta + \nu_T y, \tag{20}$$

$$M_2(y, T) = \mathbb{E}_y[V_T^2] = y^2 \nu_T^2 + 2y \nu_T (1 - \nu_T)(\theta + 1/\Lambda) + (1 - \nu_T)^2 \theta(\theta + 1/\Lambda), \tag{21}$$

where $\mathbb{E}_y[\cdot]$ is the conditional moment defined in (16). In particular, as $T \rightarrow \infty$, equations (20) and (21) yield the first two moments of the stationary diffusion V_t

$$m_1 = \mathbb{E}_\psi[V_s] = \theta \quad \text{and} \quad m_2 = \mathbb{E}_\psi[V_s^2] = \theta^2 + \theta/\Lambda. \quad (22)$$

Moreover, the stationary diffusion driven by the Heston volatility SDE has mean $m_1 = \theta$ and lagged covariances $K(u) = \mathbb{E}_\psi[V_s V_{s+u}]$ given by

$$K(u) + \theta^2 = \mathbb{E}_\psi[V_s V_{s+u}] = \mathbb{E}_\psi[V_s M_1(V_s, u)] = \mathbb{E}_\psi[V_s(1 - \nu_u)\theta + \nu_u V_s] = \theta^2 + \nu_u(m_2 - \theta^2)$$

for any time lag $u \geq 0$. This yields the stationary covariances

$$K(u) = e^{-u\kappa} \frac{\theta\gamma^2}{2\kappa} \quad \text{and} \quad K(0) = \frac{\theta\gamma^2}{2\kappa}. \quad (23)$$

6.4 Heston SDE parameters as functions of asymptotic moments

We can now express $\boldsymbol{\theta} = (\kappa, \theta, \gamma)$ as an explicit *smooth* function

$$\boldsymbol{\theta} = \Phi(m_1, K(0), K(u))$$

of three moments of the *stationary* volatility diffusion V_t , namely its mean m_1 , its variance $K(0)$, and one lagged covariance $K(u)$ for some fixed (but arbitrary) $u > 0$. Equations (22) and (23) indeed imply that parameters (κ, θ, γ) can be expressed using the moments m_1 , $K(0)$, and $K(u)$ as follows

$$\theta = m_1 = \mathbb{E}_\psi[V_t], \quad \kappa = -\frac{1}{u} \log\left(\frac{K(u)}{K(0)}\right), \quad \gamma^2 = \frac{2K(0)\kappa}{\theta}, \quad (24)$$

which defines the function Φ above.

7 Moments based observable estimators

We now use our preceding results on the Heston volatility SDEs to study a class of moment-based estimators of the Heston parameters and to discuss their consistency when the observable data are generated by the realized volatilities.

7.1 Computation of moments based observable estimators

Given the window-size $\varepsilon > 0$, select a sub-sampling time interval $\Delta \equiv \Delta(\varepsilon)$ and a number of observations $N \equiv N(\varepsilon)$. Then, the realized volatility process (2) generates an observable data set of $N(\varepsilon)$ realized volatilities

$$W_k = Y_{k\Delta(\varepsilon)}^\varepsilon, \quad k = 1 \dots N(\varepsilon).$$

Next, we specify how we use these $N(\varepsilon)$ observable data to estimate any lagged covariance $K(u)$ of the stationary diffusion V_t . Denoting $[a]_{int}$ the closest integer to a , we approximate the lag u by $U\Delta(\varepsilon)$ where

$$U = U(u, \varepsilon) = \left\lceil \frac{u}{\Delta(\varepsilon)} \right\rceil_{int} \quad \text{so that} \quad |u - U\Delta(\varepsilon)| \leq \Delta(\varepsilon). \quad (25)$$

Since $K(u)$ is Lipschitz in u , there is a constant $C \equiv C(u)$ such that

$$|K(u) - K(U\Delta(\varepsilon))| \leq C\Delta(\varepsilon) \quad \text{for all } \varepsilon > 0.$$

Then, for any ε and time lag u , we define observable empirical estimators of the mean m_1 and lagged covariances $K(u)$ of the stationary diffusion V_t as follows

$$\hat{m}^\varepsilon = \frac{1}{N} \sum_{k=1}^N W_k, \quad \hat{K}(u) \equiv \hat{K}^\varepsilon(u) = -(\hat{m}^\varepsilon)^2 + \frac{1}{N-U} \sum_{k=1}^{N-U} W_k W_{k+U}, \quad (26)$$

where $U = U(u, \varepsilon)$ and $N = N(\varepsilon)$. Formulas (24) express the parameter vector $\boldsymbol{\theta}$ as an explicit C^1 function $\Phi(m_1, K(0), K(u))$. This naturally leads to the definition of an observable parameter estimator $\hat{\boldsymbol{\theta}}(\varepsilon)$ of $\boldsymbol{\theta}$ by

$$\hat{\boldsymbol{\theta}}(\varepsilon) = \Phi(\hat{m}_1^\varepsilon, \hat{K}^\varepsilon(0), \hat{K}^\varepsilon(u)).$$

This definition yields the following explicit observable estimators of the Heston parameters

$$\hat{\theta}(\varepsilon) = \hat{m}^\varepsilon, \quad \hat{\kappa}(\varepsilon) = -\frac{1}{u} \log \left(\frac{\hat{K}^\varepsilon(u)}{\hat{K}^\varepsilon(0)} \right), \quad \hat{\gamma}^2(\varepsilon) = \frac{2\hat{K}^\varepsilon(0)\hat{\kappa}(\varepsilon)}{\hat{\theta}(\varepsilon)}. \quad (27)$$

7.2 Asymptotics for polynomial functionals of squared volatilities

Theorem 3. Consider any fixed polynomial $h(x_1, \dots, x_k)$ of total degree n in k variables (x_1, \dots, x_k) . Let $0 = u(0) < u(1) < \dots < u(k)$ be any sequence of $k+1$ lag instants. For $T > 0$, define H and H_T by

$$H = h(V_{u(1)}, \dots, V_{u(k)}) \quad \text{and} \quad H_T = h(V_{u(1)+T}, \dots, V_{u(k)+T}).$$

Recall that $\nu_T = e^{-\kappa T}$. Define $w_j = e^{-\kappa(u(j+1)-u(j))}$ for $j = 0, \dots, k-1$. Then, there is a polynomial POL in $k+2$ variables such that for all $T > 0$ and all $y > 0$

$$\mathbb{E}_y(H_T) = POL(\nu_T, y\nu_T, w_0, w_1, \dots, w_{k-1}). \quad (28)$$

The degree and coefficients of POL are determined by the integers n, k , the coefficients of h , and the vector $\boldsymbol{\theta}$. The asymptotic polynomial moments are then given by

$$\lim_{T \rightarrow \infty} \mathbb{E}_y(H_T) = \mathbb{E}_\psi(H) = POL(0, 0, w_0, w_1, \dots, w_{k-1}).$$

For any integer $q \geq 1$ there is a positive constant C , and an integer $p \geq 1$, determined only by $q, k, \boldsymbol{\theta}$ and the polynomial h such that, for all positive T and y , and all $0 = u(0) < u(1) < \dots < u(k)$

$$\left| \mathbb{E}_y[(H_T - \mathbb{E}_\psi(H))^q] \right| \leq C(1 + y^p)e^{-\kappa T}. \quad (29)$$

In particular for $q = 1$ one has

$$\left| \mathbb{E}_y(H_T) - \mathbb{E}_\psi(H) \right| \leq C(1 + y^p)e^{-\kappa T}. \quad (30)$$

Proof. For better readability, the detailed proof is given in Appendix C. □

Remarks: Equation (29) also implies that as $T \rightarrow \infty$, the random polynomial functions H_T converge in L^q -norm to the constants $\mathbb{E}_\psi(H)$, where L^q -norms are computed under \mathbb{E}_y . Note that the constant C introduced in the theorem does not depend on the time lags $u(0) < u(1) < \dots < u(k)$.

7.3 Consistency of observable estimators

Since $\hat{\boldsymbol{\theta}}(\varepsilon)$ is a C^1 function of three specific empirical moments of realized volatilities, the key consistency issue is to estimate, as $\varepsilon \rightarrow 0$, the speeds of convergence of \hat{m}_1^ε to m_1 and $\hat{K}^\varepsilon(u)$ to $K(u)$. These speeds of convergence strongly depend on the sub-sampling scheme $N(\varepsilon), \Delta(\varepsilon)$. In [11], we have determined sub-sampling schemes optimizing these speeds of convergence for *stationary* unobservable limit processes. We now prove similar results for the *non-stationary* volatilities driven by the Heston SDEs.

Theorem 4. *Consider an asset with return rate R_t and squared volatility V_t , jointly driven by the Heston SDEs (6), (7). Fix deterministic initial conditions R_0 and $V_0 = y > 0$. Call P_y the probability distribution in path space of the trajectories $\{R_t, V_t\}$. Realized volatilities Y_t^ε are computed by formula (2) with $J(\varepsilon) \sim \varepsilon^{-2}$. The Y_t^ε are sub-sampled with time step $\Delta(\varepsilon)$ to generate $N(\varepsilon)$ observations $W_k = Y_{k\Delta(\varepsilon)}^\varepsilon$. We then apply formulas (26) to compute observable empirical estimators $\hat{K}^\varepsilon(u)$ and \hat{m}^ε of the asymptotic lagged covariances $K(u) = \lim_{t \rightarrow \infty} \mathbb{E}[V_t V_{t+u}]$ and mean $m_1 = \lim_{t \rightarrow \infty} \mathbb{E}[V_t]$ of true volatilities.*

Then the optimized sub-sampling scheme

$$N(\varepsilon) \sim 1/\varepsilon \quad \text{and} \quad \Delta(\varepsilon) \sim \varepsilon^{1/2}$$

guarantees that for any fixed positive L and y there is a constant $C = C(L, y, \boldsymbol{\theta})$ such that, for all lags $0 \leq u \leq L$, one has

$$\|\hat{K}^\varepsilon(u) - K(u)\|_2 \leq C\varepsilon^{1/2} \quad \text{and} \quad \|\hat{m}^\varepsilon - m_1\|_2 \leq C\varepsilon^{1/2}, \quad (31)$$

where L^2 -norms are computed with respect to P_y . Moreover, under P_y the observable parameters estimators $\hat{\boldsymbol{\theta}}^\varepsilon$ given by formulas (27) converge in probability to the true Heston parameters $\boldsymbol{\theta}$ as $\varepsilon \rightarrow 0$. One has, for an adequate constant C ,

$$P_y \left(\|\hat{\boldsymbol{\theta}}^\varepsilon - \boldsymbol{\theta}\|_{\mathbb{R}^3} \geq \varepsilon^{1/3} \right) \leq C\varepsilon^{1/3}. \quad (32)$$

Proof. Fix the time lag u and $V_0 = y > 0$. All L^q -norms are computed under P_y . The notation “constant C ” will designate a generic constant which can change values from one bound to another. By Theorem 1, there is a constant c_4 such that for all t ,

$$\|V_t\|_4 \leq c_4 \quad \text{and} \quad \|V_t - Y_t^\varepsilon\|_2 \leq \|V_t - Y_t^\varepsilon\|_4 \leq c_4\varepsilon^{1/2}.$$

Therefore, there is a constant c_2 such that for all s and t ,

$$\|V_s V_t - Y_s^\varepsilon Y_t^\varepsilon\|_2 \leq c_2\varepsilon^{1/2}.$$

Consider the observable empirical mean and second moment estimators in (26). By subadditivity of norms, the bounds above extend to differences of empirical means to yield

$$\|\hat{m}^\varepsilon - m_1\|_2 \leq \frac{1}{N} \sum_{k=1}^N \|W_k - V_{k\Delta}\|_2 \leq C\varepsilon^{1/2}. \quad (33)$$

This proves convergence, at speed $\varepsilon^{1/2}$, of the empirical mean of realized volatilities \hat{m}^ε to the stationary mean of V_t . Next, we study our estimators of lagged covariances. Let $U = [u/\Delta(\varepsilon)]_{int}$ so that $|U\Delta - u\Delta| \leq \Delta$ and define

$$H(W) = \hat{K}^\varepsilon(u) + (\hat{m}^\varepsilon)^2 = \frac{1}{N} \sum_{k=1}^N W_k W_{k+U} \quad \text{and} \quad M(V) = \frac{1}{N} \sum_{k=1}^N V_{k\Delta} V_{(k+U)\Delta}.$$

By subadditivity of norms, we obtain

$$\|H(W) - M(V)\|_2 \leq c_2 \varepsilon^{1/2}. \quad (34)$$

Let ψ be the *stationary* density of V_t , and denote by

$$m_2(s) = \mathbb{E}_\psi[V_t V_{t+s}]$$

the stationary lagged 2nd moments, which do not depend on t . By Theorem 3, for every fixed a and $y > 0$ there is a constant C such that for all T and all $s \leq a$ one has the bound

$$\mathbb{E}_y[(V_T V_{T+s} - m_2(s))^2] \leq C e^{-\kappa T}. \quad (35)$$

The L^2 norm under P_y hence verifies

$$\|V_{j\Delta} V_{j\Delta+U} - m_2(U)\|_2 \leq C e^{-\frac{\kappa}{2} j \Delta}. \quad (36)$$

The above two bounds in (35) and (36) provide constants C and $c = \kappa/2$ such that for all ε

$$\sum_{j=1}^N \|V_{j\Delta} V_{j\Delta+U} - m_2(U)\|_2 \leq C \frac{e^{-c\Delta}}{1 - e^{-c\Delta}} \leq \frac{C}{c\Delta}. \quad (37)$$

By subadditivity of L^2 norms, inequality (37) then implies,

$$\|M(V) - m_2(U)\|_2 \leq \frac{C}{cN\Delta}. \quad (38)$$

Regrouping our definitions and notations, we have

$$\hat{K}^\varepsilon(u) = -(\hat{m}^\varepsilon)^2 + H(W), \quad K(u) = -m_1^2 + m_2(u), \quad K(U) = -m_1^2 + m_2(U).$$

This implies since $K(u)$ is Lipschitz in u ,

$$|m_2(U) - m_2(u)| = |K(U) - K(u)| \leq C|U - u| \leq C\Delta. \quad (39)$$

We have the obvious identity

$$\hat{K}^\varepsilon(u) - K(u) = H(W) - (\hat{m}^\varepsilon)^2 - (m_2(u) - m_1^2) - M(V) + M(V) - m_2(U) + m_2(U)$$

and hence

$$\|\hat{K}^\varepsilon(u) - K(u)\|_2 \leq \|m_1^2 - (\hat{m}^\varepsilon)^2\|_2 + \|H(W) - M(V)\|_2 + \|M(V) - m_2(U)\|_2 + |m_2(U) - m_2(u)|.$$

We now use the bounds (33), (34), (38), and (39) to obtain

$$\|\hat{K}^\varepsilon(u) - K(u)\|_2 \leq c_4 \varepsilon^{1/2} + c_2 \varepsilon^{1/2} + \frac{C}{cN\Delta} + C\Delta.$$

To optimize this last bound and ensure that all terms have the same rate of convergence as $\varepsilon \rightarrow 0$, we choose

$$\frac{1}{N\Delta} \sim \Delta \sim \varepsilon^{1/2}$$

which is equivalent to selecting $\Delta \sim \varepsilon^{1/2}$ and $N \sim 1/\varepsilon$.

Therefore, for each fixed $V_0 = y > 0$ and for all time lags u within any fixed interval $[0, L]$ there is then a constant C realizing the bound

$$\|\hat{K}^\varepsilon(u) - K(u)\|_2 \leq C\varepsilon^{1/2}.$$

The L^2 convergence under P_y of $\hat{K}^\varepsilon(u)$ and \hat{m}^ε to $K(u)$ and m_1 , implies their convergence in probability under P_y . By equation (27) our estimators of Heston parameters are of the form

$$\hat{\theta}^\varepsilon = \Phi(\hat{K}^\varepsilon(0), \hat{K}^\varepsilon(u), \hat{m}^\varepsilon)$$

where Φ is a C^1 function. Thus, estimators $\hat{\theta}^\varepsilon$ converge in probability to $\theta = \Phi(K(0), K(u), m_1)$ as $\varepsilon \rightarrow 0$. The L^2 -speeds of convergence $\varepsilon^{1/2}$ for the 1st and 2nd moments imply, by Chebyshev inequality,

$$P_y \left(|\hat{K}^\varepsilon(u) - K(u)| \geq \varepsilon^{1/3} \right) \leq C\varepsilon^{1/3}$$

with a similar inequality for \hat{m}^ε . Since Φ is C^1 , these speeds of convergence in probability under P_y imply, by the first order Taylor expansion of the function Φ , the same speed of convergence in probability for the parameter estimators themselves. \square

8 Optimal Partition Size $J(\varepsilon)$

The realized volatilities Y_t^ε given by the formula (2) involve averaging window of the width ε and the partition size $J(\varepsilon)$. Provided one uses the subsampling scheme

$$N(\varepsilon) \sim 1/\varepsilon, \quad \Delta(\varepsilon) \sim \varepsilon^{1/2} \tag{40}$$

and a partition size $J(\varepsilon) \sim 1/\varepsilon^2$, our current theoretical bounds can guarantee L^4 speeds of convergence $\sim \sqrt{\varepsilon}$ for $Y_t^\varepsilon - V_t$ and consistency in probability for the observable estimators of parameters in the volatility equation of the Heston model. The choice $J(\varepsilon) \sim 1/\varepsilon^2$ seems overwhelmingly large. But our numerical simulations of the Heston SDEs (see section 9.4) indicate that a more pragmatic choice $J(\varepsilon) \sim \varepsilon^{-1}$ seems to also entail $\|Y_t^\varepsilon - V_t\|_2 \sim \sqrt{\varepsilon}$ and $\|Y_t^\varepsilon - V_t\|_4 \sim \sqrt{\varepsilon}$ and consistency in probability of our observable parameter estimators.

9 Effective Speed of Convergence of realized volatilities to true volatilities

9.1 Generic stochastic volatility models versus Heston SDEs

Recall that realized volatilities Y_t^ε are computed by formula (2) with partition size $J(\varepsilon)$ for the time windows $[t - \varepsilon, t]$. Theorem 1 introduced a generic class of stochastic volatility processes V_t which were essentially assumed to have L^q -Hölder continuity with Hölder exponent $1/2$. Note that within this general class, the processes driven by the Heston SDEs (6), (7) are a very restricted subclass of diffusions. For the general class of processes, we have proved in Theorem 1 (see equation (4)) that for any fixed even integer q and for s bounded, the L^q norms $\|Y_s^\varepsilon - V_s\|_q$ must verify, for some constant C , the bounds

$$\|Y_s^\varepsilon - V_s\|_q \leq C \left(J(\varepsilon)^{1/q} + \sqrt{\varepsilon} \right). \tag{41}$$

For a more restricted class of the Heston SDEs and for the moderate partition size $J(\varepsilon) \sim 1/\varepsilon$, we conjecture that one can improve (41) to yield the following convergence speeds, valid for $q = 2, 4$ and s bounded,

$$\|Y_s^\varepsilon - V_s\|_q \sim \sqrt{\varepsilon}. \tag{42}$$

For $q = 2$, this is indeed implied by equation (41). The situation with the L^4 convergence is more complicated. Our theoretical results for the general class of diffusions in Theorem 1 seems to overestimate the size of the partition $J(\varepsilon)$ required to achieve the L^4 speed of convergence $\sim \sqrt{\varepsilon}$ in the Heston model. Since the Heston model (6), (7) is more restricted than the general class of diffusions considered in Theorem 1, a detailed analytical investigation of the Heston equations (6), (7) might yield an improved result on the L^4 convergence.

In this paper, instead of performing extensive analytical investigation of the Heston model with respect to the L^4 convergence of the realized volatility to the true volatility, we carry out simulations to validate numerically the effective L^2 and L^4 speeds of convergence of realized volatilities Y_t^ε to true volatilities V_t . Analytical investigation of the Heston model with respect to the L^4 convergence will be performed in a consequent paper.

9.2 Outline of our Heston SDEs simulations

We numerically simulate the Heston SDEs with the following specific parameters

$$\kappa = 1.7, \quad \theta = 4, \quad \gamma = 2, \quad \mu = 0.05, \quad (43)$$

and for 3 values $\beta = 0, 0.3, 0.7$ of the correlation coefficient between the Brownian noises driving the joint Heston SDEs. The Feller condition is valid since $2\kappa\theta/\gamma^2 = 3.4$. To emulate asymptotics as $\varepsilon \rightarrow 0$, we consider partition sizes

$$J(\varepsilon) = 10, 40, \varepsilon^{-1}, \varepsilon^{-2}. \quad (44)$$

and eight values $\varepsilon = 0.1, 0.05, 0.04, 0.02, 0.01, 0.008, 0.005, 0.004$ for $J(\varepsilon) = 10, 40, \varepsilon^{-1}$. For the case $J(\varepsilon) = \varepsilon^{-2}$, we consider only five values $\varepsilon = 0.1, 0.05, 0.02, 0.01, 0.005$.

Simulations of true volatility paths V_t are implemented by an Euler discretization scheme for SDEs, with time step 10^{-6} , except for $\varepsilon = 0.005$, $J(\varepsilon) = 1/\varepsilon^2$, where the time step was 1.25×10^{-7} . We perform a Grand Monte-Carlo simulation to generate a set GMC of 200,000 independent simulated paths $\{V_t, Y_t^\varepsilon\}$. Various subsets of GMC are used below for numerical estimates of specific convergence speeds.

9.3 Snapshots of joint sample paths $\{V_t, Y_t^\varepsilon\}$

For $\varepsilon = 0.01$ and $\beta = 0$, Figure 1 displays four examples of joint paths $\{V_t, Y_t^\varepsilon\}$, where realized volatilities Y_s^ε are successively computed with the four $J(\varepsilon)$ listed in (44).

Clearly, the accuracy of the approximation of V_t by Y_t^ε increases drastically for larger partition sizes $J(\varepsilon)$. The smallest $J(\varepsilon)$, equal to 10, generates many quite significant inaccuracies for $Y_t^\varepsilon - V_t$. For $J = 40$, we still note several significant inaccuracies. But for $J(\varepsilon) = 10000$ the sample paths of V_t and Y_t^ε nearly coincide. Such large partition sizes are generally not feasible: for intraday stock prices sampled every minute, a partition size $J = 10000$ would require an unrealistic sliding time window of about 20 trading days. For small values of $J(\varepsilon)$, a practical remedy to eliminate large sharp peaks of $|Y_t^\varepsilon - V_t|$ is time smoothing of the Y_t^ε either directly, or by using a weighted average in (2).

9.4 Numerical Asymptotics of $\|Y_t^\varepsilon - V_t\|_q$ as $\varepsilon \rightarrow 0$

We partition our set GMC of 200,000 simulated paths into 200 disjoint subsets GMC_k of $MC = 1000$ paths each. We now fix $T = 1$, and for each GMC_k , $k = 1, \dots, 200$, the empirical mean $M_k(q)$

Snapshots of V_t and Y_t^ε for $\varepsilon=0.01$ and $J=10, 40, 1/\varepsilon, 1/\varepsilon^2$

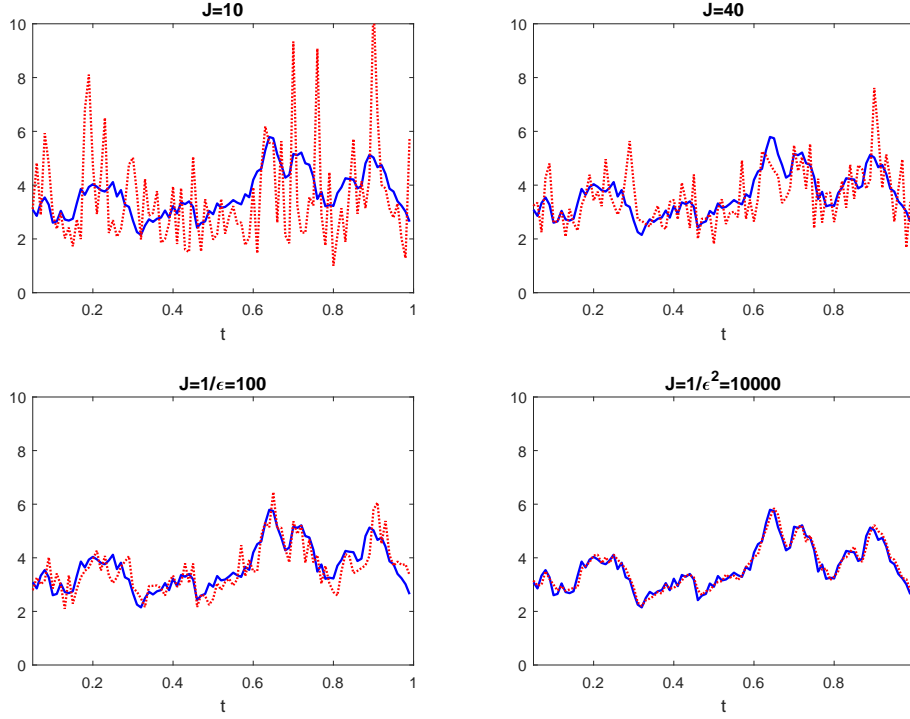


Figure 1: Volatility V_t and Realized Volatility Y_t^ε snapshots for $\varepsilon = 0.01$ and four partition sizes $J = J(\varepsilon)$ as in (44). Each sub-plot displays in solid blue the time evolution of one single random trajectory of the volatility V_t , $0 \leq t \leq 1$ and displays in dotted red an associated random time evolution of the realized volatility Y_t^ε . Parameters in the Heston volatility SDEs are as in (43). The two Heston SDEs are here driven by Brownian motions with zero correlation $\beta = 0$.

of $|Y_T^\varepsilon - V_T|^q$ over the 1000 paths (in the corresponding subset GMC_k) provides an estimator $\hat{l}_k^q = (M_k(q))^{1/q}$ for the L^q errors $\|Y_T^\varepsilon - V_T\|_q$. Final estimates for these L^q errors are then given by

$$\hat{L}^q = \frac{1}{200} \sum_{k=1}^{200} \hat{l}_k^q, \quad (45)$$

with 95% confidence intervals $\hat{L}^q \pm 1.96\sigma(q)$ where

$$\sigma^2(q) = \frac{1}{200} \sum_{k=1}^{200} \left(\hat{l}_k^q - \hat{L}^q \right)^2.$$

For the constant partition sizes $J(\varepsilon) = 10$ and $J(\varepsilon) = 40$, the upper parts of Figures 2 and 3 display error estimates \hat{L}^2 and \hat{L}^4 computed via (45). These error estimates are nearly constant with negligible decreases as $\varepsilon \rightarrow 0$. Note that \hat{L}^2 as well \hat{L}^4 errors are both approximately twice smaller for $J = 40$ than for $J = 10$. For $q = 2$, this is correctly predicted by our theoretical bound (4). But for $q = 4$, our theoretical bound is too pessimistic, since it predicts that \hat{L}^4 should be about 1.4 times smaller for $J = 40$ than for $J = 10$. For the partition sizes $J(\varepsilon) = 1/\varepsilon$ and $J(\varepsilon) = 1/\varepsilon^2$, our numerical results are displayed in the bottom sub-plots of Figures 2 and 3, and they do support the following conjecture about the limiting behavior (as $\varepsilon \rightarrow 0$) of the L^4 error

$$\|Y_t^\varepsilon - V_t\|_4 \sim \left(J(\varepsilon)^{-1/2} + \varepsilon^{1/2} \right). \quad (46)$$

$\varepsilon =$	0.005	0.01	0.02	0.05	0.1
$\hat{L}^2, J = 1/\varepsilon$	0.45	0.64	0.90	1.39	1.94
$\hat{L}^4, J = 1/\varepsilon$	0.71	1.01	1.41	2.20	3.09
$\hat{L}^2, J = 1/\varepsilon^2$	0.16	0.23	0.34	0.57	0.90
$\hat{L}^4, J = 1/\varepsilon^2$	0.23	0.32	0.48	0.83	1.34

Table 1: Values of estimated \hat{L}^2 and \hat{L}^4 errors as defined in (45) in numerical simulations with $J(\varepsilon) = 1/\varepsilon$ and $J(\varepsilon) = 1/\varepsilon^2$.

This conjecture is also confirmed by Figure 4 where for both $J(\varepsilon) = \varepsilon^{-1}$ and $J(\varepsilon) = \varepsilon^{-2}$, the log-log scale plots of \hat{L}^2 and \hat{L}^4 follow nearly perfect straight lines with slope 1/2 as soon as ε is small enough. Thus these results demonstrate quite convincingly that errors scale according to $\hat{L}^2 \sim \hat{L}^4 \sim \varepsilon^{1/2}$ for both $J(\varepsilon) \sim \varepsilon^{-1}$ and $J(\varepsilon) \sim \varepsilon^{-2}$. Therefore our simulations indicate that for $q = 2$ and $q = 4$ convergence speeds $\|Y_t^\varepsilon - V_t\|_q \sim \sqrt{\varepsilon}$ can be achieved for fixed t when the realized volatility Y_t^ε is computed with partition sizes $J(\varepsilon) \sim \varepsilon^{-1}$. This also implies that for the partition size $J(\varepsilon) \sim \varepsilon^{-1}$ lagged covariances of realized volatilities should converge to true lagged covariances at L^2 -speeds $\sim \sqrt{\varepsilon}$. Therefore in further numerical simulations below, we will systematically use the pragmatic sub-sampling scheme

$$N(\varepsilon) \sim 1/\varepsilon, \quad \Delta(\varepsilon) \sim \varepsilon^{1/2}, \quad J(\varepsilon) \sim 1/\varepsilon. \quad (47)$$

We have performed additional simulations with $\beta = 0.3$ and $\beta = 0.7$, where β is the correlation between the two noises driving the joint Heston SDEs. Our numerical results with $\beta > 0$ are almost identical to those for $\beta = 0$, as indicated by the log-log plots in Figures 5 and 6.

This is consistent with our proof of Theorem 1, which explores the autonomous Heston SDE (7) driving the true volatility V_t , without ever using the Heston SDE (6) for the rate of return process. Another key ingredient of our proof is the study of conditional expectations $\mathbb{E}(Y|X)$ when X and Y are polynomial functions of a finite number of V_t values. Again this analysis does not use the Heston SDE (6). Constants introduced in Theorem 1 may depend on β , but our numerical simulations indicate that this dependence is fairly weak.

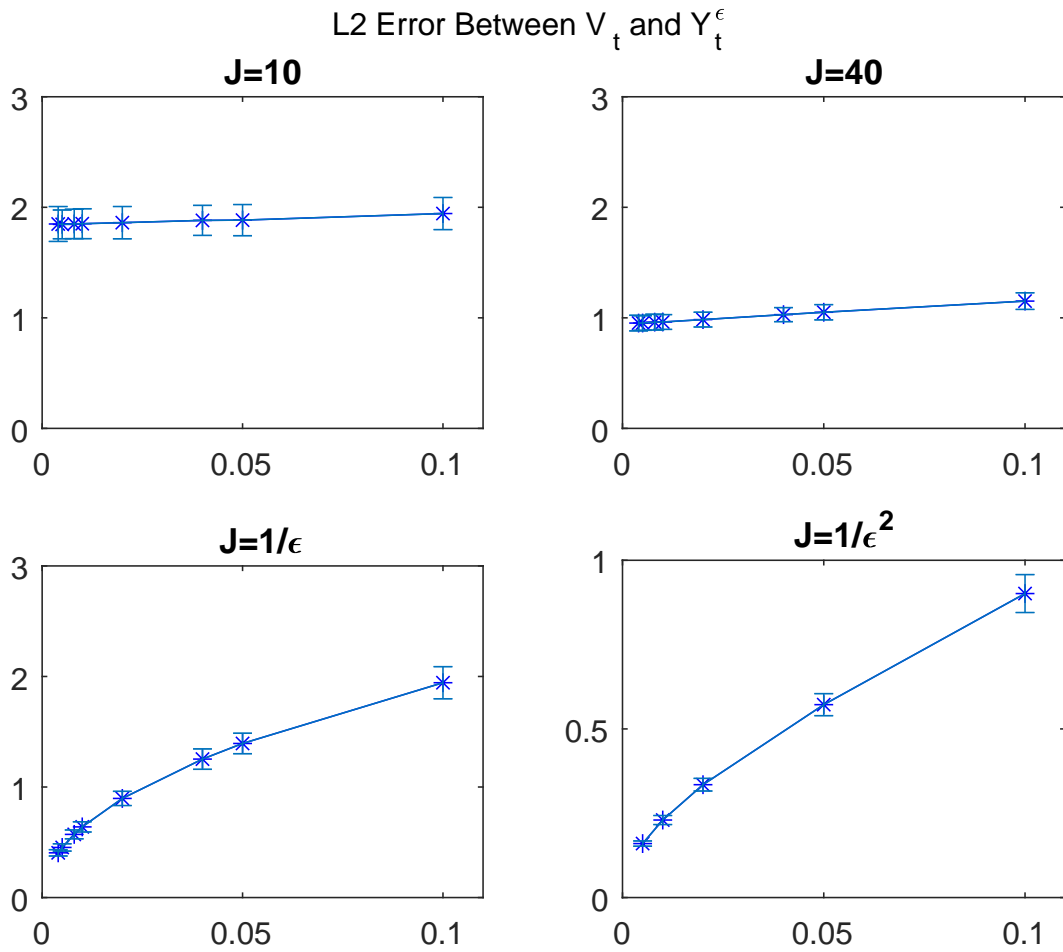


Figure 2: Simulations of the Heston SDEs with $\beta = 0$ and parameters listed in (43) and partition sizes in (44). We depict numerical estimates for the L^2 errors $\|Y_T^\epsilon - V_T\|_2$ with $T = 1$, with error bars identifying 95% confidence intervals.

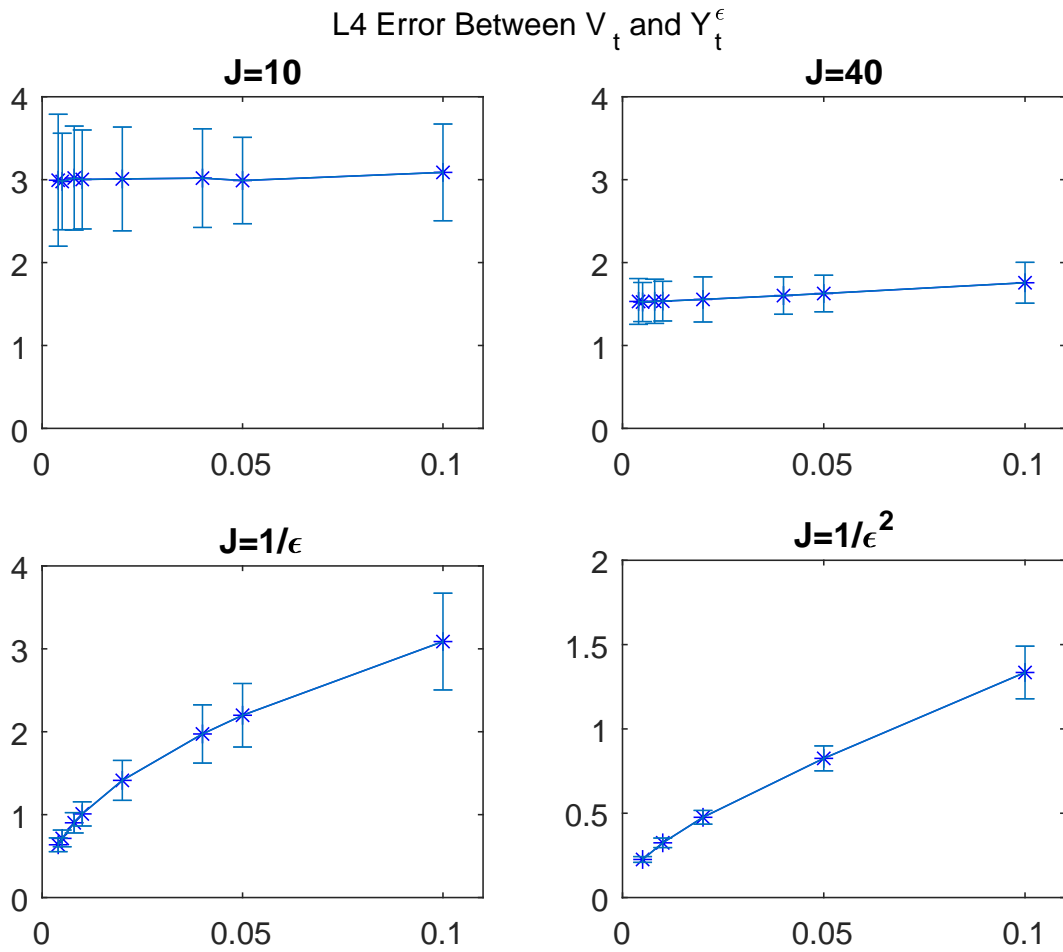


Figure 3: Simulations of the Heston SDEs with $\beta = 0$ and parameters listed in (43) and partition sizes in (44). We depict numerical estimates for the L^4 errors $\|Y_T^\epsilon - V_T\|_4$ with $T = 1$, with error bars identifying 95% confidence intervals.

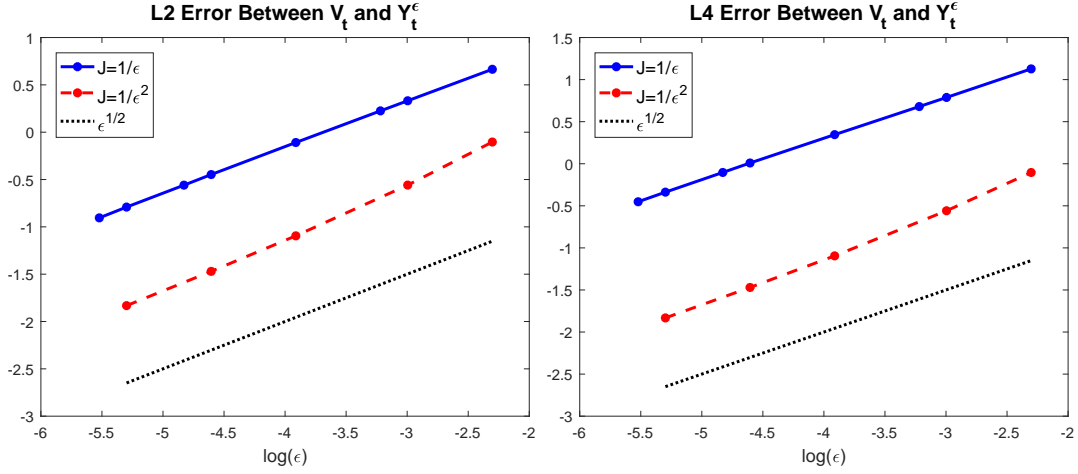


Figure 4: Simulations of the Heston SDEs with $\beta = 0$ and parameters listed in (43). Log-log plots of L^2 and L^4 errors for $T = 1$. We plot $\log(\hat{L}^2)$ on the left sub-plot and $\log(\hat{L}^4)$ on the right sub-plot, as functions of $\log(\epsilon)$, for the partition sizes $J(\epsilon) = \epsilon^{-1}$ (solid blue line) and $J(\epsilon) = \epsilon^{-2}$ (dashed red line). The dotted black line represents a reference line with the slope $1/2$.

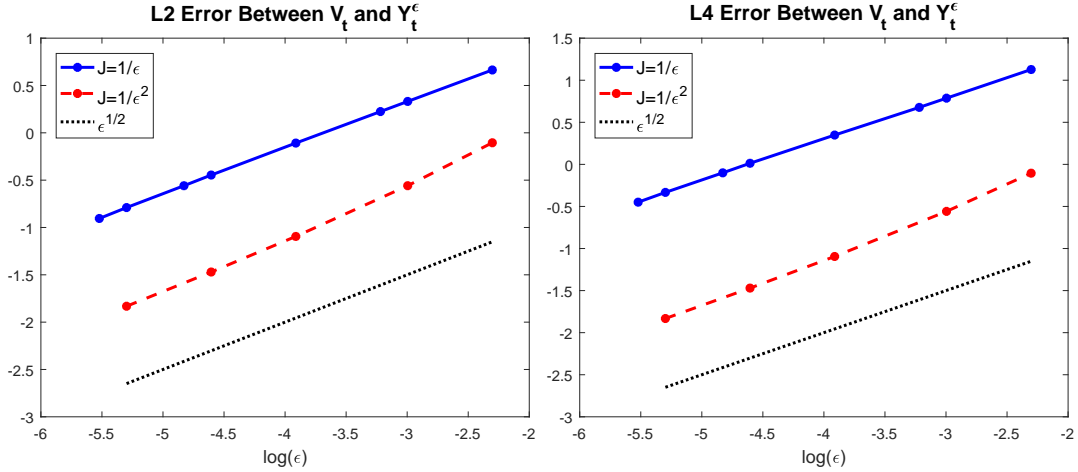


Figure 5: Simulations of the Heston SDEs with $\beta = 0.3$ and parameters listed in (43). Log-log plots of L^2 and L^4 errors for $T = 1$. We plot $\log(\hat{L}^2)$ on the left sub-plot and $\log(\hat{L}^4)$ on the right sub-plot, as functions of $\log(\epsilon)$, for the partition sizes $J(\epsilon) = \epsilon^{-1}$ (solid blue line) and $J(\epsilon) = \epsilon^{-2}$ (dashed red line). The dotted black line represents a reference line with the slope $1/2$.

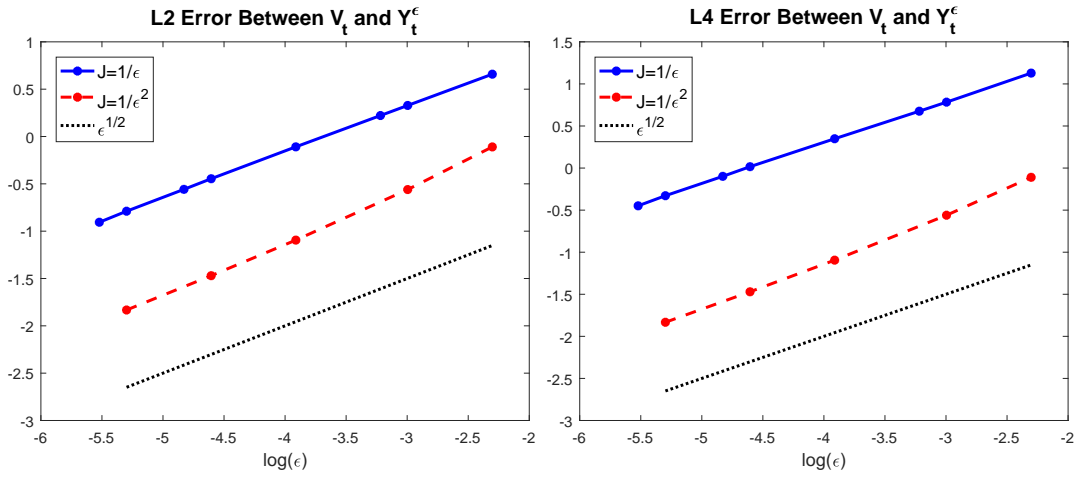


Figure 6: Simulations of the Heston SDEs with $\beta = 0.7$ and parameters listed in (43). Log-log plots of L^2 and L^4 errors for $T = 1$. We plot $\log(\hat{L}^2)$ on the left sub-plot and $\log(\hat{L}^4)$ on the right sub-plot, as functions of $\log(\epsilon)$, for the partition sizes $J(\epsilon) = \epsilon^{-1}$ (solid blue line) and $J(\epsilon) = \epsilon^{-2}$ (dashed red line). The dotted black line represents a reference line with the slope $1/2$.

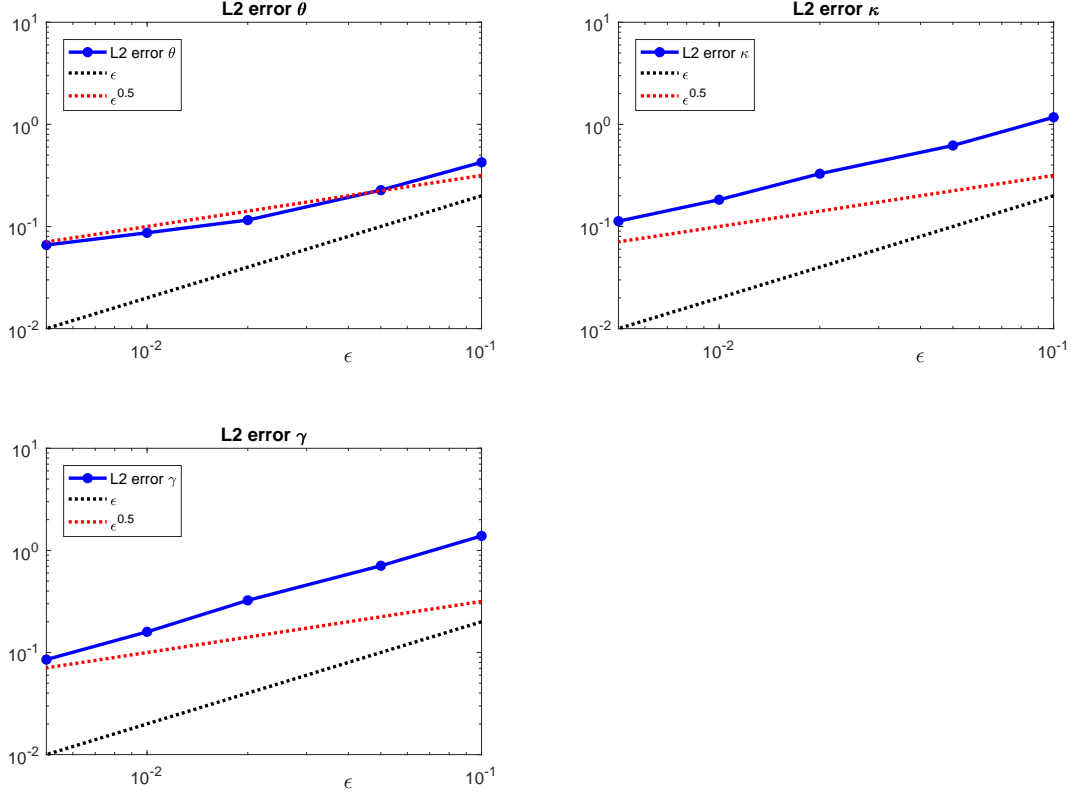


Figure 7: Log-log plots of numerical L_2 -errors for parameter estimators of the Heston volatility SDE. We plot, as functions of $\log(\varepsilon)$, the logarithms of $\|\hat{\theta}^\varepsilon - \theta\|_2$ (top left panel, blue solid line), $\|\hat{\kappa}^\varepsilon - \kappa\|_2$ (top right panel, blue solid line), $\|\hat{\gamma}^\varepsilon - \gamma\|_2$ (bottom left panel, blue solid line). In all plots red dotted line and black dotted line represent straight reference lines with slopes $1/2$ and 1 , respectively.

10 Effective convergence speeds for observable estimators of Heston parameters

In this section we evaluate numerical convergence speeds for our observable estimators $\hat{\theta}_\varepsilon$, $\hat{\kappa}_\varepsilon$, $\hat{\gamma}_\varepsilon$ of the Heston volatility SDE parameters. This set of simulations is performed as outlined in section 9.2 with the following five values of $\varepsilon = 0.1, 0.05, 0.02, 0.01, 0.005$. Realized volatilities are computed with the pragmatic partition sizes $J(\varepsilon) = \varepsilon^{-1}$. In order to compute estimators we use the sup-sampling regime $N(\varepsilon) = 100\varepsilon^{-1}$, $\Delta(\varepsilon) = 1/\sqrt{\varepsilon}$, which is a particular case of our general theoretical recipe in (47). Numerical estimates for the L^2 errors for parameter estimators are computed using a Monte-Carlo approach with 1000 long trajectories consistent with the sub-sampling regime outlined above. Each long trajectory yields one set of estimated parameter values computed using (27).

The lag u^ε is chosen to be approximately 0.6. However, since in discrete formulas the lag is a multiple of Δ , i.e. $u^\varepsilon = l \times \Delta(\varepsilon)$ the lag changes slightly for different values of ε . The values of the lag for simulations with different values of ε are chosen to be $u^\varepsilon = [0.62, 0.66, 0.56, 0.6, 0.568]$.

Numerical estimates for the L^2 -errors of parameter estimators are presented in Figure 7. We note first that $\|\hat{\theta}^\varepsilon - \theta\|_2 \sim \sqrt{\varepsilon}$ as could be expected since $\hat{\theta}_\varepsilon$ is the empirical mean of the sub-sampled Y_t^ε . In particular, linear regression gives the convergence rate $\|\hat{\theta}^\varepsilon - \theta\|_2 \sim \varepsilon^{0.6}$. Moreover,

Figure 7 indicates that the L^2 -errors $\|\hat{\kappa}^\varepsilon - \kappa\|_2$ and $\|\hat{\gamma}^\varepsilon - \gamma\|_2$ both tend to zero at much faster speeds. Linear regression for these two parameters gives the rates of convergence $\|\hat{\kappa}^\varepsilon - \kappa\|_2 \sim \varepsilon^{0.77}$ and $\|\hat{\gamma}^\varepsilon - \gamma\|_2 \sim \varepsilon^{0.93}$.

These numerical results suggest that the generic convergence speeds $\sim \sqrt{\varepsilon}$ proved in Theorem 4 could be improved to speeds close to $\sim \varepsilon$ for the observable estimators of κ and γ , even when realized volatilities are computed with the pragmatic partition sizes $J(\varepsilon) \sim \varepsilon^{-1}$. Note that $\hat{\kappa}^\varepsilon$ and $\hat{\gamma}^\varepsilon$ are explicit C^1 functions which involve ratios of observable moment estimators (see (27)). Therefore, faster speeds of convergence for $\hat{\kappa}^\varepsilon$ and $\hat{\gamma}^\varepsilon$ can be potentially explained by correlated errors in the numerator and denominator of the corresponding formulas in (27).

10.1 Numerical convergence speeds for the mean and lagged covariances of realized volatilities

Limiting behavior of observable estimators of the Heston parameters κ and γ strongly depends on the behavior of lagged covariances $K^\varepsilon(u)$ of Y_t^ε . In the previous section, we demonstrated that numerical speeds of convergence for $\hat{\kappa}^\varepsilon$ and $\hat{\gamma}^\varepsilon$ are faster than $\sqrt{\varepsilon}$. In this section we use simulations of the Heston SDEs to investigate numerically the convergence of empirical moments estimators $K^\varepsilon(0)$ and $K^\varepsilon(u)$ as $\varepsilon \rightarrow 0$. Simulation parameters are identical to the ones reported in section 10.

We focus here on two time lags $u = 0$ and $u \approx 0.6$. The mean and lagged covariances of Y_t^ε are approximated by their empirical estimators, given by

$$\hat{m}^\varepsilon = \frac{1}{N} \sum_{j=1}^N Y_{j\Delta}^\varepsilon, \quad \hat{K}^\varepsilon(u) = \frac{1}{N-s} \sum_{i=1}^{N-s} Y_{i\Delta}^\varepsilon Y_{(i+s)\Delta}^\varepsilon - (\hat{m}^\varepsilon)^2, \quad (48)$$

where integer s is chosen to be $s = 0$ (lag $u = 0$) and such that $s\Delta \approx 0.6$ (lag $u \approx 0.6$). Recall the stationary moments of true volatilities (22), (23) given by

$$m = \lim_{t \rightarrow \infty} \mathbb{E}(V_t) = \theta, \quad K(u) = \lim_{t \rightarrow \infty} \text{cov}(V_t V_{t+u}) = \frac{\theta \gamma^2}{2\kappa} e^{-\kappa u}. \quad (49)$$

We approximate the L^2 -errors of \hat{m}^ε and $\hat{K}^\varepsilon(u)$ by the empirical means

$$\|\hat{m}^\varepsilon - m\|_2 \equiv \sqrt{\frac{1}{MC} \sum_{k=1}^{MC} (\hat{m}^\varepsilon - m)^2}, \quad (50)$$

$$\|\hat{K}^\varepsilon(u) - K(u)\|_2 \equiv \sqrt{\frac{1}{MC} \sum_{k=1}^{MC} \left(\hat{K}^\varepsilon(u) - K(u) \right)^2}, \quad (51)$$

where the two sums involve $MC = 1000$ independent evaluations of $\hat{K}^\varepsilon(u)$ and \hat{m}^ε . L^2 accuracy of observable moment estimators in (50) and (51) are impacting directly the numerical accuracy of our observable estimators of the Heston SDEs parameters.

For $u = 0$ and $u \approx 0.6$ we then compute the empirical L^2 estimates specified by (50), (51). These results are displayed in Figure 8. We observe that with the partition size $J(\varepsilon) = \varepsilon^{-1}$ we obtain speeds of convergence roughly comparable to $\sqrt{\varepsilon}$. In particular, linear regression on $\log(\varepsilon)$ for the three moments of Y_t^ε displayed in Figure 8 indicate the following speed of convergence for the mean $\|\hat{m}^\varepsilon - m\|_2 \sim \varepsilon^{0.6}$, and speeds of convergence for the second moments are given approximately by $\|\hat{K}^\varepsilon(0) - K(0)\|_2 \sim \varepsilon^{0.8}$ and $\|\hat{K}^\varepsilon(u^\varepsilon) - K(u^\varepsilon)\|_2 \sim \varepsilon^{0.4}$. Slightly slower speed of convergence of the lagged moment estimator $\hat{K}^\varepsilon(u^\varepsilon)$ can be potentially improved by selecting a larger value of $N(\varepsilon)$.

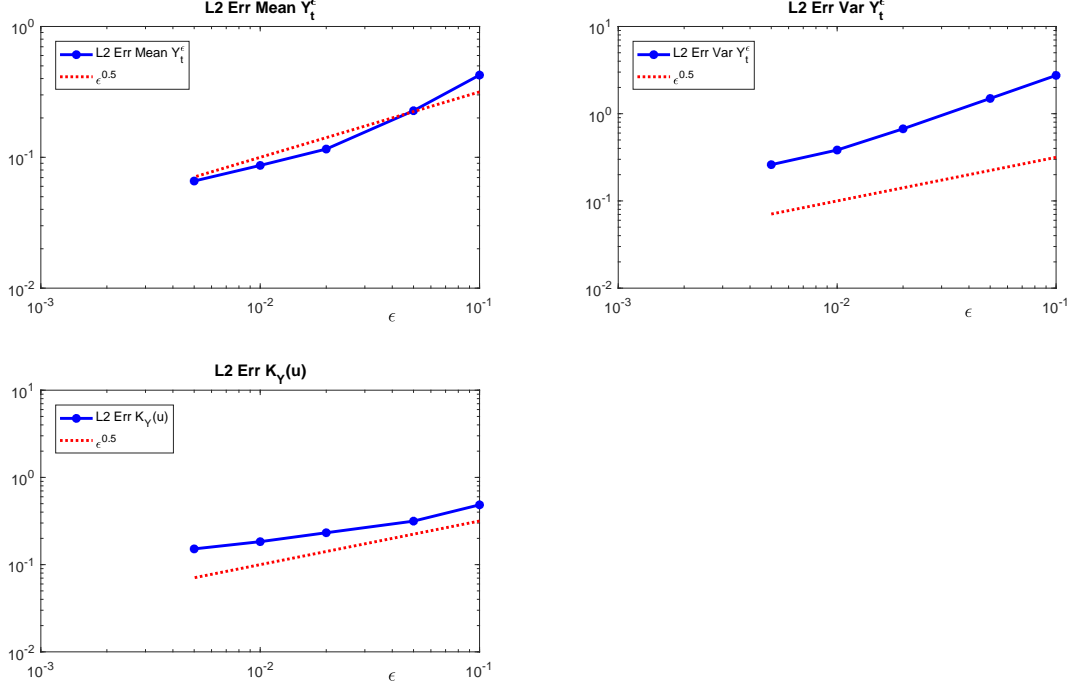


Figure 8: Log-log plots for L^2 estimation errors for moments of Y_t^ε , computed by equations (50) and (51). Graphs are plotted as functions of $\log(\varepsilon)$. Top left panel - $\log \|\hat{m}^\varepsilon - m\|_2$, top right panel - $\log \|\hat{K}^\varepsilon(0) - K(0)\|_2$, bottom left panel - $\log \|\hat{K}^\varepsilon(u) - K(u)\|_2$ with $u \approx 0.6$.

Our numerical simulations indicate that it should be possible to improve analytical results for the convergence of empirical covariances of the realized volatility process and observable parameter estimators. In particular, we expect that we should be able to obtain convergence rates $\sim \sqrt{\varepsilon}$ for the empirical covariances of the realized volatility under a much more realistic sub-sampling regime $J(\varepsilon) \sim \varepsilon^{-1}$. Moreover, since the convergence rates for $\hat{\kappa}^\varepsilon$ and $\hat{\gamma}^\varepsilon$ are much faster than the convergence rates of the observable moments estimators (especially of \hat{m}^ε and $\hat{K}^\varepsilon(u^\varepsilon)$), we conjecture that estimation errors in observable moments estimators are positively correlated and thus first order terms practically cancel in the Taylor expansions of the nonlinear functions which define $\hat{\kappa}$ and $\hat{\gamma}$ in (27).

The choice of the lag u^ε is motivated by some practical considerations. In particular, one should perform an a-posteriori check after the parameter estimator $\hat{\kappa}$ is computed and ensure that the correlation function is in the appropriate range, e.g. $e^{-\hat{\kappa}u^\varepsilon} \in [0.3, 0.7]$. Apart from the practical constraint above, the choice of u^ε is otherwise arbitrary. We performed numerical simulations (not reported here) investigating several other choices of the lag u^ε . In particular, we considered $u^\varepsilon \approx 0.3$ and the “vanishing lag” case $u^\varepsilon = \Delta \equiv \sqrt{\varepsilon}$. Our numerical simulations indicate that the choice $u^\varepsilon \approx 0.6$ produces near-optimal asymptotic behavior of both, observable moment estimators and parameter estimators themselves.

11 Conclusions

We carried out an extensive analytical and numerical investigation of the Heston joint SDEs driving jointly the volatilities V_t and the rate of returns R_t . Since the volatility process V_t cannot be observed directly, realized volatilities Y_t^ε computed from the R_τ with τ in the sliding window

$[t - \varepsilon, t]$ are classical observable approximations of the unobservable V_t .

The main goal of this paper is to define and study observable estimators of the Heston SDEs parameters, computable from the Y_t^ε , and exhibiting asymptotic consistency as $\varepsilon \rightarrow 0$. This context fits general frameworks of *indirect observability* where parameter estimators for the dynamics of an unobservable process X_t can only be computed from observations of a process Y_t^ε approximating X_t as $\varepsilon \rightarrow 0$. Computing realized volatilities Y_t^ε from the rates of returns R_t requires partitioning the window $[t - \varepsilon, t]$ into $J(\varepsilon)$ time intervals. For the Heston SDEs we apply our general theory of indirect observability to prove precise bounds for L^q norms $\|Y_t^\varepsilon - V_t\|_q$ in terms of $J(\varepsilon)$ and ε . In particular we show that $\|Y_t^\varepsilon - V_t\|_4 \leq C\sqrt{\varepsilon}$ provided $J(\varepsilon) \sim 1/\varepsilon^2$. However, partition sizes $J(\varepsilon) \sim 1/\varepsilon^2$ are not very practical since they require an overwhelming number of points for small window sizes, ε . Our numerical simulations indicate that similar speeds of convergence should still hold for more practical partition sizes $J(\varepsilon) \sim 1/\varepsilon$.

Our observable estimators of the Heston SDEs parameters are defined as an explicit function of the empirical mean and two empirical lagged covariances computed from $N(\varepsilon)$ observations $Y_{j\Delta(\varepsilon)}^\varepsilon$, $j = 1, \dots, N(\varepsilon)$ of the realized volatility, sub-sampled with time step $\Delta(\varepsilon)$. We prove that for fastest convergence speed of observable parameter estimators to true parameters, a nearly optimal sub-sampling regime is provided by $N(\varepsilon) \sim 1/\varepsilon$ and $\Delta(\varepsilon) \sim 1/\sqrt{\varepsilon}$ with $J(\varepsilon) \sim 1/\varepsilon^2$. Again our simulations of the Heston SDEs indicate that partition sizes $J(\varepsilon) \sim 1/\varepsilon$ combined with our nearly optimal sub-sampling regime $N(\varepsilon) \sim 1/\varepsilon$, $\Delta(\varepsilon) \sim 1/\sqrt{\varepsilon}$ achieve adequate L^2 -speeds of convergence ($\sim \sqrt{\varepsilon}$ or faster) for the observable parameter estimators.

Numerical simulations of the Heston SDEs presented in this paper provide practical guidelines for an adequate choice of the averaging window, ε , to compute realized volatilities and parameter estimators, in order to fit the Heston SDEs to practical observations of stock prices. We intend to explore this strategy on several choices of one-minute financial data in a future paper.

Acknowledgements. I.T. and R.A. were supported in part by the NSF Grant DMS-1109582. I.T. is also partially supported by the NSF Grant DMS-1620278.

A Hölder continuity in L^q for a certain class of diffusions

We prove here that trajectories of processes driven by SDEs with drift and spot variance in L^q are Hölder continuous in L^q , with Hölder coefficient $1/2$.

Proposition 3. *Let Z_t be a standard Brownian motion and denote \mathcal{F}_t the increasing filtration generated by the process Z_t . Let x_t be a process starting with x_0 in L^q and driven by the SDE*

$$dx_t = b_t dt + \sigma_t dZ_t,$$

where the drift b_t and the coefficient $\sigma_t \geq 0$ are progressively measurable with respect to the filtration \mathcal{F}_t . Let $v_t = \sigma_t^2$. Fix an integer $q \geq 2$ and a time $T \geq 0$. Assume that the L^q -norms $\|b_t\|_q$ and $\|v_t\|_q$ remain bounded for $t \leq T$. Then there is then a constant C such that, for all $0 \leq s \leq t \leq T$

$$\|x_t - x_s\|_q \leq C\sqrt{t-s} \text{ and } \|x_t\|_q \leq C. \quad (52)$$

When the drift b_t is identically zero, we have a more precise inequality for all $0 \leq s \leq t$

$$\|x_t - x_s\|_q \leq S_{q-1}\sqrt{t-s}, \quad (53)$$

where S_q is defined by

$$S_q = S_q(s, t) = \sup_{s \leq u \leq t} \sqrt{\|v_u\|_q} = \sup_{s \leq u \leq t} \|\sigma_u\|_{2q}.$$

Proof. Equation (52) is an easy consequence of equation (53). Hence, we only need to focus on proving (53) in the case of zero drift $b_t = 0$, so that $dx_u = \sigma_u dZ_u$. Fix $s \leq t$ so that the $S_q = S_q(s, t)$ are also fixed in the proof. The Itô isometry implies

$$\|x_t - x_s\|_2 = \left[\int_s^t \mathbb{E}[\sigma_u^2] du \right]^{1/2} \leq S_1(t-s)^{1/2},$$

which proves (53) for $q = 2$. Proceed by recurrence and assume that (53) is already proved for some $r \geq 2$. Consider the process $g_u = x_u - x_s$ with $s \leq u \leq t$. By Itô formula the process g_u^{r+1} verifies the following SDE

$$d(g_u^{r+1}) = (r+1)g_u^r \sigma_u dZ_u + r(r+1)/2 g_u^{r-1} v_u du.$$

Integrating and taking expectations, we obtain

$$\mathbb{E}[g_t^{r+1}] = r(r+1)/2 \int_s^t \mathbb{E}[g_u^{r-1} v_u] du. \quad (54)$$

Set $p = \frac{r}{r-1}$ so that $1/p + 1/r = 1$. By duality between L^p and L^r ,

$$\left| \mathbb{E}[g_u^{r-1} v_u] \right| \leq \|g_u^{r-1}\|_p \|v_u\|_r = \|g_u\|_r^{r-1} \|v_u\|_r \leq \|g_u\|_r^{r-1} S_r^2. \quad (55)$$

Our recurrence hypothesis allows to apply (53) to $\|g_u\|_r$, so that using the inequality $S_{r-1} \leq S_r$, the last equation becomes

$$\left| \mathbb{E}[g_u^{r-1} v_u] \right| \leq S_r^2 S_{r-1}^{r-1} (u-s)^{(r-1)/2} \leq S_r^{r+1} (u-s)^{(r-1)/2}.$$

Substituting the last expression in (54) and integrating in u we obtain

$$\mathbb{E}[g_t^{r+1}] \leq S_r^{r+1} (t-s)^{(r+1)/2}.$$

Raising this to the power $1/(r+1)$, we obtain the bound in L^{r+1}

$$\|x_t - x_s\|_{r+1} \leq S_r (t-s)^{1/2},$$

which concludes the proof by recurrence. \square

B Proof of Theorem 1

Recall the statement of Theorem 1: Consider a generic stochastic volatility model where asset prices A_t with return rate R_t and squared volatility $V_t > 0$ are linked by the SDE (1) driven by a Brownian motion Z_t . The volatilities V_t are assumed to be progressively measurable with respect to the filtration \mathcal{F}_t , where \mathcal{F}_t is generated by V_0 and the Z_s , $0 \leq s \leq t$. Fix an integer $q \geq 2$ and a time $T > 0$, and note that the following results hold for T finite as well as for $T = +\infty$.

Assume that there is a constant c such that, for all $0 \leq s \leq t < T$,

$$\|V_t\|_q \leq c \text{ and } \|V_t - V_s\|_q \leq c(t-s)^{1/2}. \quad (56)$$

Define

$$\bar{q} = \begin{cases} q & q \text{ is even} \\ q+1 & q \text{ is odd.} \end{cases}$$

Then there is a constant C such that for any partition size function $J(\varepsilon)$, the realized squared volatilities Y_t^ε given by (2) verify, for all $\varepsilon > 0$

$$\|Y_t^\varepsilon - V_t\|_q \leq C \left(\frac{1}{J^{1/\bar{q}}(\varepsilon)} + \sqrt{\varepsilon} \right) \text{ for all } t < T. \quad (57)$$

Since $\lim_{\varepsilon \rightarrow 0} J(\varepsilon) = +\infty$, the realized volatilities Y_t^ε converge in L^q to the true volatilities V_t as $\varepsilon \rightarrow 0$, at uniform speed for $t < T$. By selecting $J(\varepsilon) = \varepsilon^{-\bar{q}/2}$, one can achieve an L^q -speed of convergence proportional to $\sqrt{\varepsilon}$, i.e. there is a constant $C_q = C(q, T)$ such that

$$\|Y_t^\varepsilon - V_t\|_q \leq C_q \sqrt{\varepsilon} \text{ for all } t < T, \varepsilon > 0. \quad (58)$$

Proof. Recall that for any random variables W_1, \dots, W_q in L^q , one has

$$|\mathbb{E}[W_1 W_2 \dots W_q]| \leq \|W_1\|_q \|W_2\|_q \dots \|W_q\|_q \quad (59)$$

as is easily seen by recurrence, using Hölder inequality.

Fix T and q . By Proposition 3 there is a constant C such that

$$\|R_t\|_q \leq C \text{ and } \|R_t - R_s\|_q \leq C(t-s)^{1/2} \text{ for all } 0 \leq s \leq t \leq T. \quad (60)$$

Once equation (57) is proved for $\mu = 0$, it is easily extended to arbitrary μ values. Hence, we will assume $\mu = 0$, so that $dR_t = \sqrt{V_t} dZ_t$. Using Itô formula, we can define random variables $D(s, t)$ by

$$D(s, t) = (R_t - R_s)^2 - \int_s^t V_u du = 2 \int_s^t w_u dZ_u \text{ with } w_u = (R_u - R_s) V_u^{1/2} \quad (61)$$

so that

$$\mathbb{E}[D(s, t) | \mathcal{F}_s] = 2\mathbb{E} \left[\int_s^t w_u dZ_u \right] = 0 \text{ for } s \leq t. \quad (62)$$

For $0 \leq s \leq u \leq t \leq T$, equation (60) and the hypothesis on $\|V_u\|_q$ provide a constant C_1 such that

$$\|R_u - R_s\|_{2q} \leq C_1 \sqrt{u-s} \text{ and } \|V_u\|_q \leq C_1.$$

By Cauchy inequality

$$\mathbb{E}[|w_u|^q] \leq \|(R_u - R_s)^q\|_2 \|V_u^{q/2}\|_2$$

and hence, setting $C_2 = C_1^2$, we obtain

$$\|w_u\|_q \leq \|R_u - R_s\|_{2q} \|V_u\|_q \leq C_2(u - s)^{1/2}.$$

Applying (53) to $x_u = D(s, u)$ we obtain

$$\|D(s, t)\|_q = 2 \left\| \int_s^t w_u dZ_u \right\|_q \leq 2C_2 \int_s^t (u - s)^{1/2} du = C_2(t - s). \quad (63)$$

For each $\varepsilon > 0$, select an integer $J = J(\varepsilon)$ and consider the time points $t_n = t - \varepsilon + n\varepsilon/J$, with $n = 0, \dots, J$, to define the realized volatilities by

$$Y_t^\varepsilon = \sum_{n=1}^J (R_{t_n} - R_{t_{n-1}})^2. \quad (64)$$

Next, introduce random variables

$$U_n = D(t_{n-1}, t_n) = (R_{t_n} - R_{t_{n-1}})^2 - \int_{t_{n-1}}^{t_n} V_u du = 2 \int_{t_{n-1}}^{t_n} w_u dZ_u \quad (65)$$

which due to equation (63) verify

$$\|U_n\|_q \leq C_2(t_n - t_{n-1}) = C_2 \frac{\varepsilon}{J}. \quad (66)$$

We now define

$$H(t, \varepsilon) = Y_t^\varepsilon - \frac{1}{\varepsilon} \int_{t-\varepsilon}^t V_u du \quad \text{and} \quad K(t, \varepsilon) = \frac{1}{\varepsilon} \int_{t-\varepsilon}^t V_u du - V_t \quad (67)$$

in order to write

$$Y_t^\varepsilon - V_t = H(t, \varepsilon) + K(t, \varepsilon). \quad (68)$$

By the definitions of U_n and Y_t^ε in (65) and (64), respectively, we have

$$H(t, \varepsilon) = Y_t^\varepsilon - \frac{1}{\varepsilon} \int_{t-\varepsilon}^t V_u du = \frac{1}{\varepsilon} \sum_{n=1}^J U_n. \quad (69)$$

Assume from now on that the integer q is *even*, and define the polynomial Q by

$$Q = \left(\sum_{n=1}^J U_n \right)^q.$$

Since q is even, we have $\mathbb{E}[|H(t, \varepsilon)|^q] = \mathbb{E}[H(t, \varepsilon)^q]$ and hence equation (69) entails

$$\|H(t, \varepsilon)\|_q = \frac{1}{\varepsilon} (\mathbb{E}[Q])^{1/q}. \quad (70)$$

Let $M = M(q, J)$ be the set of multi-integers

$$m = (m(1), \dots, m(q)) \quad \text{with all } m(k) \in [1, J].$$

For $m \in M$ denote by Q_m the monomial $Q_m = U_{m(1)}U_{m(2)} \cdots U_{m(q)}$. We now expand the polynomial Q as follows

$$Q = \left(\sum_{n=1}^J U_n \right)^q = \sum_{m \in M} Q_m.$$

For each $m \in M$, let $m^* = \max(m(1), \dots, m(q))$ and let $z(m)$ be the number of indexes $m(k)$ such that $m(k) = m^*$. For $1 \leq r \leq q$, call M_r the set of $m \in M$ such that $z(m) = r$. Then M is the disjoint union of the q subsets M_r . Each multi-index $m \in M_r$ contains at most $q - r + 1$ distinct indexes $m(k)$, with $m(k)$ ranging from 1 to J , hence each M_r has cardinal $Card(M_r) \leq J^{q-r+1}$. For $r \geq 2$ this yields $Card(M_r) \leq J^{q-1}$, and then

$$Card(M - M_1) = \sum_{r=2}^{r=q} Card(M_r) \leq (q-1)J^{q-1}.$$

Using property (59) and equation (66), we have for all $m \in M$

$$\mathbb{E}[|Q_m|] \leq \|U_{m(1)}\|_q \cdots \|U_{m(q)}\|_q \leq C_3 \frac{\varepsilon^q}{J^q},$$

where $C_3 = C_2^q$. Since $Card(M - M_1) \leq (q-1)J^{q-1}$, we have

$$\left| \sum_{m \in M - M_1} \mathbb{E}[Q_m] \right| \leq C_3 Card(M - M_1) \frac{\varepsilon^q}{J^q} \leq (q-1)C_3 \frac{\varepsilon^q}{J}. \quad (71)$$

For $m \in M_1$, the integer $m^* = \max(m(1) \dots m(q))$ is reached by a single index $m(r) = j$ with $2 \leq j \leq J$. We can then reorder m as a multi-index p verifying

$$p(1) \leq p(2) \leq \dots \leq p(q-1) \leq (j-1) < p(q) = j.$$

Let $s = t_{j-1}$ and $t = t_j$. Due to equation (62) and to the definition of the U_n , we have

$$\mathbb{E}[U_j | \mathcal{F}_s] = \mathbb{E}[D(s, t) | \mathcal{F}_s] = 0.$$

For $1 \leq k \leq q-1$ all the $U_{p(k)}$ are \mathcal{F}_s -measurable, so that for all $m \in M_1$

$$\mathbb{E}[Q_m] = \mathbb{E}[U_{p(1)} \cdots U_{p(q-1)} U_{p(q)}] = \mathbb{E}[U_{p(1)} \cdots U_{p(q-1)} \mathbb{E}(U_{p(q)} | \mathcal{F}_s)] = 0$$

which yields $\mathbb{E}[Q] = \sum_{m \in M - M_1} \mathbb{E}[Q_m]$. Equation (71) now implies

$$\mathbb{E}[Q] = |\mathbb{E}[Q]| \leq (q-1)C_3 \frac{\varepsilon^q}{J}.$$

In view of equation (70), we now obtain the bound

$$\|H(t, \varepsilon)\|_q = \frac{1}{\varepsilon} (\mathbb{E}[Q])^{1/q} \leq C_4 \frac{1}{J^{1/q}},$$

where $C_4 = ((q-1)C_3)^{1/q} \leq 2C_2$.

We now study $K(t, \varepsilon)$ defined by (67), which we rewrite as

$$K(t, \varepsilon) = \frac{1}{\varepsilon} \int_{t-\varepsilon}^t (V_u - V_t) du.$$

This implies

$$\|K(t, \varepsilon)\|_q \leq \frac{1}{\varepsilon} \int_{t-\varepsilon}^t \|V_t - V_u\|_q du.$$

By hypothesis on the volatility process V_t , there is a constant C_5 such that for $u \leq t \leq T$ one has $\|V_t - V_u\|_q \leq C_5(t-u)^{1/2}$ and hence

$$\|K(t, \varepsilon)\|_q \leq \frac{C_5}{\varepsilon} \int_{t-\varepsilon}^t (t-u)^{1/2} du = \frac{2}{3} C_5 \varepsilon^{1/2}.$$

Therefore, for q even, there is then a constant $C = \max(C_4, C_5)$ such that for all $t \leq T$ and all $\varepsilon > 0$

$$\|Y_t^\varepsilon - V_t\|_q \leq \|H(t, \varepsilon)\|_q + \|K(t, \varepsilon)\|_q \leq C \left(\frac{1}{J^{1/q}} + \varepsilon^{1/2} \right)$$

which concludes the proof. \square

C Polynomial functions of volatilities and Theorem 3

We evaluate conditional moments for polynomial functions of squared volatilities. Note that conditioning by the σ -algebras \mathcal{F}_s gives the same results for the stationary diffusion V_t and for the process V_t starting at any fixed $V_0 = y > 0$.

Theorem 3 was stated as follows in the main text: Fix any polynomial h of total degree n in k variables (x_1, \dots, x_k) . Let $0 = u(0) < u(1) < \dots < u(k)$ be any sequence of $k+1$ lag instants. For $T > 0$, define H and H_T by

$$H = h(V_{u(1)}, \dots, V_{u(k)}) \quad \text{and} \quad H_T = h(V_{u(1)+T}, \dots, V_{u(k)+T}). \quad (72)$$

Recall that $\nu_T = e^{-T\kappa}$. Define $w_j = e^{-\kappa(u(j+1)-u(j))}$ for $j = 0, \dots, k-1$. There is then a polynomial POL in $k+2$ variables such that for all $T > 0$ and all $y > 0$

$$\mathbb{E}_y(H_T) = POL(\nu_T, y\nu_T, w_0, w_1, \dots, w_{k-1}). \quad (73)$$

The degree and coefficients of POL are determined by the integers n, k , the coefficients of h , and the vector $\boldsymbol{\theta}$. The asymptotic polynomial moments are then given by

$$\lim_{T \rightarrow \infty} \mathbb{E}_y(H_T) = \mathbb{E}_\psi(H) = POL(0, 0, w_0, w_1, \dots, w_{k-1}).$$

For any integer $q \geq 1$ there is a positive constant C , and an integer $p \geq 1$, determined only by $q, k, \boldsymbol{\theta}$ and the polynomial h such that, for all positive T and y , and all $0 = u(0) < u(1) < \dots < u(k)$

$$\left| \mathbb{E}_y [|H_T - \mathbb{E}_\psi(H)|^q] \right| \leq C(1 + y^p) e^{-T\kappa}. \quad (74)$$

In particular for $q = 1$ one has

$$\left| \mathbb{E}_y(H_T) - \mathbb{E}_\psi(H) \right| \leq C(1 + y^p) e^{-T\kappa}. \quad (75)$$

Remarks: Equation (74) also implies that as $T \rightarrow \infty$, the random polynomial functionals H_T converge in L^q -norm to the constants $\mathbb{E}_\psi(H)$, where L^q -norms are computed under \mathbb{E}_y . Note also, that all the constants introduced in the theorem and in its proof below do not depend on the actual lag instants $u(0) < u(1) < \dots < u(k)$.

Proof of Theorem 3:

Proof. By linearity, we only need to consider the case when h is a monomial in k variables. For $k = 1$, the result was proved by (17). Proceeding by recurrence on k , assume the result is true for monomials in $k - 1$ variables (x_2, \dots, x_k) . Any monomial h in k variables can be written as $h = x_1^m g(x_2, \dots, x_k)$. Define

$$G_T = g(V_{u(2)+T}, \dots, V_{u(k)+T}) \quad \text{and} \quad H_T = V_{u(1)+T}^m G_T.$$

The recurrence hypothesis provides a polynomial R in $(k + 1)$ variables such that, for all T

$$\mathbb{E}_y(G_T) = R(\nu_T, y\nu_T, w_1, w_2, \dots, w_{k-1})$$

where the coefficients of R are determined by g, θ . By the Markov property we thus get

$$\mathbb{E}(G_T | \mathcal{F}_{u(1)+T}) = R(\nu_T, V_{u(1)+T} \nu_T, w_1, w_2, \dots, w_{k-1}).$$

Since $\mathbb{E}_y[H_T] = \mathbb{E}_y[V_{u(1)+T}^m \mathbb{E}(G_T | \mathcal{F}_{u(1)+T})]$ we then obtain

$$\mathbb{E}_y[H_T] = \mathbb{E}_y \left[V_{u(1)+T}^m R(\nu_T, V_{u(1)+T} \nu_T, w_1, w_2, \dots, w_{k-1}) \right].$$

Each monomial M of R is of the form $\nu_T^p (V_{u(1)+T} \nu_T)^j S(w_1, w_2, \dots, w_{k-1})$ for some p, j and some polynomial S . Then in the right-hand side of (73), M contributes a term of the form

$$\Gamma(M) = \nu_T^{p+j} S(w_1, w_2, \dots, w_{k-1}) \mathbb{E}_y \left[V_{u(1)+T}^{m+j} \right].$$

Due to (17) with $q = m + j$, this last conditional expectation is a polynomial in the two variables

$$\nu_{u(1)+T} = \nu_T w_0 \quad \text{and} \quad V_0 \nu_{u(1)+T} = y \nu_T w_0$$

with coefficients depending only on $m + j$ and θ . Hence $\Gamma(M)$ is a polynomial in ν_T and $y\nu_T$, with coefficients which are polynomials in $(w_0, w_1, w_2, \dots, w_{k-1})$, fully determined by m, j, θ . The same property must then hold for the sum $\mathbb{E}_y(H_T)$ of all the $\Gamma(M)$ contributed by the monomials M of R . This completes the proof of (73) by recurrence on k .

Write POL in (73) as a polynomial $POL(z)$ in the $k + 2$ variables z_i . The vector $z(T) = (\nu_T, y\nu_T, w_0, \dots, w_{k-1})$ tends to $z(\infty) = (0, 0, w_0, \dots, w_{k-1})$ as $T \rightarrow \infty$. The polynomial $Q(z(T)) = POL(z(T)) - POL(z(\infty))$ can be written for some integer p

$$Q(z(T)) = \nu_T A_0 + \sum_{s=1}^p y^s \nu_T^s A_s,$$

where for $s = 0, \dots, p$, each A_s is a polynomial in the $(k + 1)$ variables $(\nu_T, w_0, \dots, w_{k-1})$. Since all these positive $(k + 1)$ variables are inferior to 1, then each $|A_s|$ remains bounded for all $T \geq 0$ and all $u(0) < u(1) < \dots < u(k)$. Hence there is a constant C such that

$$|A_s| \leq C \quad \text{and} \quad y^s \leq C(1 + y^p) \quad \text{for all } s = 0, \dots, p, T \geq 0, y > 0.$$

For all $s \geq 1$ we have $\nu_T^s \leq \nu_T = e^{-T\kappa}$, and hence the expansion of $Q(z(T))$ provides a new constant C_1 such that, for all $u(0) < u(1) < \dots < u(k)$,

$$|\mathbb{E}_y(H_T) - \mathbb{E}_\psi(H)| = |Q(z(T))| \leq C_1(1 + y^p)e^{-T\kappa} \quad \text{for all } T \geq 0, y > 0.$$

This proves (75).

Let $\bar{H} = \mathbb{E}_\psi(H)$. Expand $\beta(T) = (H_T - \bar{H})^q$ as a linear combination of terms of the form $\bar{H}^{q-j} H_T^j$ for $j = 0, \dots, q$. Recall that h is a polynomial in x_1, x_2, \dots, x_k . For j fixed, $\sigma_j = h^j$ is also a polynomial in x_1, x_2, \dots, x_k . By definition (72), we can express both $\Sigma = H^j$ and $\Sigma_T = H_T^j$ as

$$\Sigma = \sigma_j (V_{u(1)}, \dots, V_{u(k)}) \quad \text{and} \quad \Sigma_T = \sigma_j (V_{u(1)+T}, \dots, V_{u(k)+T}).$$

For each j , equation (75) applied to the polynomial $\sigma = h^j$ provides a constant C_j and an integer $p(j)$ such that

$$\left| \mathbb{E}_y(\Sigma_T) - \mathbb{E}_\psi(\Sigma) \right| \leq C_j \left(1 + y^{p(j)} \right) e^{-T\kappa} \quad \text{for all } T \geq 0, y > 0$$

and hence there are constants c_j such that

$$\left| \mathbb{E}_y(\bar{H}^{q-j} H_T) - \mathbb{E}_\psi(\bar{H}^{q-j} H_T) \right| \leq c_j \left(1 + y^{p(j)} \right) e^{-T\kappa} \quad \text{for all } T \geq 0, y > 0.$$

Applying this to $j = 0, \dots, q$ and using the Newton binomial formula yields, for some new constant C ,

$$\mathbb{E} [|\beta(T)|] \leq C e^{-T\kappa} \sum_{j=0}^q c_j \left(1 + y^{p(j)} \right) \quad \text{for all } T \geq 0, y > 0$$

which completes the proof of (74). □

References

- [1] Y. Aït-Sahalia. Maximum likelihood estimation of discretely sampled diffusions: a closed-form approximation approach. *Econometrica*, 70(1):223–262, 2002.
- [2] Y. Aït-Sahalia. Closed-form likelihood expansions for multivariate diffusions. *Ann. Statist.*, 36(2):906–937, 04 2008.
- [3] Y. Aït-Sahalia and R. Kimmel. Maximum likelihood estimation of stochastic volatility models. *Journal of Financial Economics*, 83(2):413–452, 2007.
- [4] Y. Aït-Sahalia, P. Mykand, and L. Zhang. How often to sample a continuous-time process in the presence of market microstructure noise. *Review of Fiancancial Stuides*, 18(2):315–416, 2005.
- [5] Y. Aït-Sahalia, P. Mykand, and L. Zhang. A tale of two time scales. *Journal of the American Statistical Association*, 100(472):1394–1411, 2005.
- [6] S. Alizadeh, M. W. Brandt, and F. X. Diebold. Range-based estimation of stochastic volatility models. *The Journal of Finance*, 57(3):1047–1091, 2002.
- [7] R. Azencott, A. Beri, A. Jain, and I. Timofeyev. Sub-sampling and parametric estimation for multiscale dynamics. *Comm. Math. Sci.*, 11(4):939–970, 2013.
- [8] R. Azencott, A. Beri, and I. Timofeyev. Adaptive sub-sampling for parameteric estimation of Gaussian diffusions. *J. Stat. Phys.*, 139(6):1066–1089, 2010.

- [9] R. Azencott, A. Beri, and T. Timofeyev. Parametric estimation of stationary stochastic processes under indirect observability. *J. Stat. Phys*, 144(1):150–170, 2011.
- [10] R. Azencott and Y. Gadhyan. Accurate parameter estimation for coupled stochastic dynamics. In *DCDS Special Issue, Proc. 7th AIMS Conf. “Dyn. Syst. and Diff. Eq.”*, pages 44–53. AIMS, 2009.
- [11] R. Azencott, P. Ren, and I. Timofeyev. Parametric estimation from approximate data: Non-Gaussian diffusions. *J. Stat. Phys.*, 161(5):1276–1298, 2015.
- [12] F. Bandi and J. Russell. Separating microstructure noise from volatility. *Journal of Financial Econometrics*, 79(3):655–692, 2006.
- [13] O. Barndorff-Nielsen and N. Shephard. Econometric analysis of realized volatility and its use in estimating stochastic volatility models. *Journal of the Royal Statistical Society, Series B*, 64:253–280, 2002.
- [14] I. V. Basawa and B. Prakasa Rao. *Statistical Inference for Stochastic Processes*. London and New York: Academic Press, 1980.
- [15] D. S. Bates. Maximum likelihood estimation of latent affine processes. *Review of Financial Studies*, 19(3):909–965, 2006.
- [16] K. Christensen, R. Oomen, and M. Podolskij. Realised quantile-based estimation of the integrated variance. *Journal of Econometrics*, 159:74–98, 2010.
- [17] K. Christensen, M. Podolskij, and M. Vetter. Bias-correcting the realized rangebased variance in the presence of market microstructure noise. *Finance and Stochastics*, 13:239–268, 2009.
- [18] J. Cox, J. Ingersoll, and R. Ross. A theory of the term structure of interest rates. *Econometrica*, pages 385–408, 1985.
- [19] D. Crommelin and E. Vanden-Eijnden. Diffusion estimation from multiscale data by operator eigenpairs. *Multiscale Modeling & Simulation*, 9(4):1588–1623, 2011.
- [20] D. Duffie and K. J. Singleton. Simulated moments estimation of markov models of asset prices. *Econometrica*, 61(4):929–952, 1993.
- [21] W. Feller. The asymptotic distribution of the range of sums of independent random variables. *Annals of Mathematical Statistics*, 22(3):427–432, 1951.
- [22] V. Genon-Catalot. Maximmm contrast estimation for diffusion processes from discrete observations. *Statistics*, 21(1):99–116, 1990.
- [23] V. Genon-Catalot, T. Jeantheau, C. Laredo, et al. Parameter estimation for discretely observed stochastic volatility models. *Bernoulli*, 5(5):855–872, 1999.
- [24] S. L. Heston. A closed-form solution for options with stochastic volatility with applications to bond and currency options. *Review of financial studies*, 6(2):327–343, 1993.
- [25] I. Kalnina. Subsampling high frequency data. *Journal of Econometrics*, 161(2011):262–283, 2010.

- [26] F. Mariani, G. Pacelli, and F. Zirilli. Maximum likelihood estimation of the heston stochastic volatility model using asset and option prices: an application of nonlinear filtering theory. *Optimization Letters*, 2(2):177–222, 2008.
- [27] A. Papavasiliou, G. A. Pavliotis, and A. Stuart. Maximum likelihood drift estimation for multiscale diffusions. *Stoch. Proc. and Applics.*, 119(10):3173–3210, 2009.
- [28] G. A. Pavliotis and A. Stuart. Parameter estimation for multiscale diffusions. *J. Stat. Phys.*, 127:741–781, 2007.
- [29] P. C. B. Phillips and J. Yu. *Maximum Likelihood and Gaussian Estimation of Continuous Time Models in Finance*, pages 497–530. Springer Berlin Heidelberg, Berlin, Heidelberg, 2009.
- [30] E. Ruiz. Quasi-maximum likelihood estimation of stochastic volatility models. *Journal of Econometrics*, 63(1):289 – 306, 1994.